Analyses of fast neutron inelastic scattering cross sections to higher (vibrational) states of ^{232}Th and ^{238}U. II. Intrinsic unified formalism

D. W. S. Chan* and E. Sheldon
Department of Physics and Applied Physics, University of Lowell, Lowell, Massachusetts 01854
(Received 26 March 1982)

From the standpoint of nuclear theory, the consistency of the unified (statistical S matrix) formalism, even in its most basic form as treated in this paper, represents a fundamental improvement over the standard approach involving the incoherent addition of compound-nucleus and direct-interaction contributions to a net angle-integrated cross section. A previous paper dealt with standard analyses of ^{232}Th(n,n') and ^{238}U(n,n') level excitation functions from threshold to $E_n=2.5$ MeV, and foreshadowed the successful application of the unified formalism in illustrative analyses of (n,n') scattering to triads of $K=0^-$ octupole vibrational states in each of the above nuclei. For these deformed actinide nuclei, a coupled-channels treatment is appropriate: The unified approach intrinsically entails this as a central feature. This paper describes the results of such unified computations for the ^{232}Th and ^{238}U scattering cross sections to each of 21 principal collective (quadrupole and octupole vibrational) states in ^{232}Th up to $E^*=1208.7$ keV, and to 17 such levels in ^{238}U up to $E^*=1269.4$ keV, using the relative coupling strengths as the only adjustable parameter. When compared with the measured data, the unified fits were generally of equivalent or superior quality to those derived from the standard treatment, with the same (Bruyères) optical potential parameters employed throughout. Comparisons with (composite) evaluated neutron data file values reveals discrepancies which indicate an evident need for reevaluation. Corrections to the basic unified data will be considered in a subsequent paper.

[NUCLEAR REACTIONS ^{232}Th(n,n') and ^{238}U(n,n'), $E_n=0.8-2.5$ MeV; measured, calculated, and evaluated $\sigma(E_n)$. Theoretical $\sigma(n,n')$ computed for vibrational states with unified (statistical S-matrix) formalism. Compared with experimental, standard theoretical, and composite evaluated level excitation-function data.]

I. OVERVIEW

As was shown in the previous paper[1] (hereafter designated as paper I), the standard theoretical approach of building level excitation functions for ^{232}Th(n,n') and ^{238}U(n,n') processes by incoherent summation of compound-nuclear (CN) and coupled-channels direct-interaction (DI) cross sections was capable of providing reasonably good fits in most instances to the energy variation of cross sections measured by the Lowell group from threshold to 2.5 MeV for some 21 vibrational states in ^{232}Th and 17 in ^{238}U. These constituted the lowest members of $K=0$, 1, 2, and 3 quadrupole and octupole vibrational bands built upon the $K=0$ ground-state rotational band. Details of the experimental procedures were given in paper I; the standard theoretical approach was also described therein and a foretaste of the unified approach was provided in preliminary calculations applied to three members of the $K=0$ octupole bands in ^{232}Th and ^{238}U: The results indicated that the unified formalism was potentially able to furnish fits to the experimental data that were of equivalent or improved quality. It is the purpose of this paper to explore the capabilities of this unified statistical S-matrix treatment as an alternative to the standard approach, and also to indicate the extent of deviation that the Evaluated Nuclear Data File (ENDF-B/V) data evince when compared with experimental, standard theoretical, or unified theoretical excitation functions for groups of combined levels.

II. BACKGROUND

Ever increasing recognition has been given to the importance for the safe and effective design and operation of fission reactors, and especially for fast breeder reactors, of assembling an accurate, comprehensive, and reliable precision data base concerning the detailed variation with energy of the neutron scattering cross section for the actinide nuclei, and particularly for the principal even-even actinides, ^{232}Th and ^{238}U, for which considerable effort has been invested in the measurement and calculation of elastic and inelastic cross sections over the energy range from threshold to several MeV. The energy spectrum for a typical fast breeder reactor is such that about one-third of the neutron flux lies above 1 MeV; since the inelastic scattering is primarily responsible for the slowing-down rate of the fission neutrons, the shape of the spectrum is crucially determined by the composite scattering behavior. Although the needs of reactor designers, operators, and engineers can be met to a large extent by order-of-magnitude bulk data devoid of fine detail, the macroscopic approach to data acquisition is not only theoretically inadmissible, but suffers from the lack of accurate predictive capability in situations that are inaccessible to experimental verification. For valid quantitative conclusions to be drawn in regard to cross-section information, the theoretical alternative of a detailed, methodical determination over a reasonable energy range, under known and well-controlled conditions that permit valid interpolation and extrapolation, offers a more justifiable basis. Thereby, the discriminating evaluator is provided with an altogether more dependable foundation from which to proceed: By judicious combination of the requisite elements from a microscopic approach a more reliable and finely-tuned conclusion in regard to macroscopic data can be drawn.

The energy dependence of the scattering follows complicated trends, owing in part to the intricate nuclear energy-level schemes of the involved nuclei and due also to the interplay between the interaction mechanisms that mediate the scattering. The level schemes of the actinide nuclei such as ^{232}Th and ^{238}U evince a densely-packed, collective character, with quadrupole and octupole vibrational multiplets built upon rotational bands, as depicted in Figs. 1 (a) and (b). The deformed collective nature of such target nuclei suggests that coupled-channels direct interaction is likely to make a significant contribution to the net scattering process, an expectation that is clearly borne out by the experimental findings.[1–3] The standard theoretical treatment that takes cognizance of these influences level by level is, as described in paper I, to evaluate the compound-nuclear (CN) cross section, using the Hauser-Feshbach-Moldauer formalism in a statistical computer code such as CINDY,[4] which makes provision for competition from extra outgoing (neutron) channels, and to combine this incoherently (i.e., by simple addition) with the strong-coupling direct-interaction (DI) cross section determined by a coupled-equations program such as JUPITOR[5] or its Karlsruhe variant KARJUP,[6] in which up to six levels from various collective bands can be coupled simultaneously. For consistency, a uniform set of optical potential and deformation parameters, as determined by the Bruyères group,[7] has been retained throughout the entire batch of computations, leaving the relative coupling strengths as the only adjustable parameters in the calculations. The optical potential used in papers I and II is of the conventional derivative Woods-Saxon type with Thomas-form spin-orbit coupling, whose well parameters are (in the customary notation, with E_n denoting the laboratory energy of the projectile):

$$V = V_0 - 0.3E_n \text{ MeV}; \quad W = 3.6 + 0.4E_n \text{ MeV};$$
$$r_0 = r_0' = 1.26 \text{ fm}, \quad a = 0.63 \text{ fm}, \quad a' = 0.52 \text{ fm};$$
$$V_{so} = 6.2 \pm 0.3 \text{ MeV}, \quad (r_0)_{so} = 1.12 \text{ fm}, \quad a_{so} = 0.47 \text{ fm}, \tag{1}$$

where $V_0 = 46.4 \pm 0.2$ MeV, and the ground-state deformation parameters are $\beta_2 = 0.190$ and $\beta_4 = 0.071$ for ^{232}Th, while $V_0 = 46.2 \pm 0.2$ MeV, and $\beta_2 = 0.198$ and $\beta_4 = 0.057$ for ^{238}U. The resulting level excitation functions, as presented in paper I, demonstrate that this approach yields satisfactory fits in the majority of instances. In certain remaining cases of discrepancy, it may be that the experimental data are incorrect, due to errors in the allowances made for γ cascading, internal conversion, and/or pronounced secondary structure in the γ-emission angular distribution (i.e., inordinately large higher-order terms in the Legendre polynomial expansion) when (n,n') cross sections are deduced from $(n,n'\gamma)$ γ-production yield measurements. Alternatively, some of the remanent discrepancies may be attributed to insufficient correction for multiple scattering, or to the absence of correction for the effects of competing fission channels (in supplementary calculations, the influence of continuum competition and of radiative capture was found to be only slight).

Of more fundamental significance from the

theoretical standpoint, however, is the fact that the standard approach is based upon intensity addition, rather than amplitude addition, and so fails to take proper account of possible interaction between the CN and DI components in arriving at an overall cross section for the process. The treatment is essentially incoherent. Although coupling of channels is incorporated within the formalism, the interaction of the contributants to the reaction is not adequately allowed for. This basic shortcoming is avoided in the unified approach, which sets out from the statistical S-matrix ensemble, comprising the entire set of transition elements, as the repository of the essential physics in the problem. The underlying formalism has been developed by Weidenmüller *et al.*[8–12] following the inception of the Engelbrecht-Weidenmüller transformation[8] in 1973. This more intricate approach can be applied to pure CN processes in the form of an "extended Hauser-Feshbach" theory, or, with further elaboration, can be formulated to include DI components in a unified scheme which takes phase relationships into account and so allows for a systematic, comprehensive coupled-channels treatment.

When first put forward, the formalism was tested only in a quantitatively synthetic manner, in that random S-matrix theory was employed in an examination[10] of the basic features of this approach. Subsequently, an explicit numerical application was undertaken by the Erlangen group[13,14] in a study of ^{90}Zr$(\vec{p},p'\gamma)$ isoanalog resonance data. Assisted by special simplifying conditions, the theoretical treatment could be reduced to a less complex, and thereby more tractable, form, in that drastic reductions in the number and type of scattering channels enabled the calculations to be performed with a fairly elementary program, FLIPPER,[14] entailing only 34 K storage capacity and nonlengthy runs. Developed from the DWBA T-matrix code RENATE,[15] which itself had been compiled from the universally used DI code DWUCK,[16] this did not allow for the DI channel-coupling procedures that are inherent in the present calculations. Because of the simplifications, it was possible to carry out the calculations in a formalism that entailed summation over magnetic quantum numbers characterizing the transitions, thereby essentially describing the scattering process through the formation and decay of nuclear magnetic substates.[17] The analyses embodied three categories of interaction, namely

(i) CN processes, treated as "fluctuation" phenomena in "absorption" channels proceeding via $T_<$ compound states in the intermediate nucleus ^{91}Nb;

(ii) off-resonance DI processes, evaluated with T-matrix DWBA procedures, without channel coupling, as described above; and

(iii) on-resonance direct inelastic scattering from the 0^+ ground state of ^{90}Zr to the 2^+ second excited state at $E^*=2.18$ MeV: This was treated as exclusively due to the population and decay of the $T_>$ isoanalog states in ^{91}Nb, having spin $\frac{3}{2}^+$ and, for incident protons in the 6–9 MeV range, lying at excitation energies between $E^*=12$ and 14 MeV in the continuum region. Four such $T_>$ isoanalog states, serving as doorway states for the neighboring $T_<$ states, were included in the calculations. Their decay to the 2^+ second excited state in ^{90}Zr involved $s_{1/2}$, $d_{3/2}$, $d_{5/2}$, and $g_{7/2}$ partial waves, associated with the $d_{3/2}$ incident wave.

Since the presence of a DI component induces nonstatistical correlations in the individual reaction channels of the compound nucleus, especially if the DI process occurs as a doorway mechanism,[18,19] it is to be expected that compound states with the same $(\frac{3}{2}^+)$ spin as the isoanalog states would be preferentially excited, causing a resonancelike enhancement of the CN scattering cross section for the $\frac{3}{2}^+$ compound contribution from the above partial waves. Thus, even in the simplified regime, it is necessary to consider five sets of contributions to the theoretical cross section in the resonance region, namely

(a) a small and fairly uniform pure DWBA direct contribution;

(b) a rather larger, but again fairly uniform off-resonant CN contribution (the "off-resonance background absorption");

(c) a resonantly-peaked CN contribution from the $\frac{3}{2}^+$ intermediate $T_<$ states;

(d) a substantial, dominant, direct scattering component from the four $T_>$ isoanalog states responsible for the resonance; and

(e) a small enhancement, discernible primarily at the resonance peak, due to constructive interference between the direct isoanalog resonance scattering and the pure DI background.

The measured (energy-averaged) cross section data of the Erlangen group[20,21] exhibited resonances at 6.81, 7.66, and 7.86 MeV incident proton energy. Previous analyses by Lieb *et al.*[22] had indicated that a substantial part of the cross section could be attributed to CN scattering in the resonance region; however, the existence of appreciable polarization[23] in the scattered beam indicated the presence of direct processes, originally attributed to the influence of the second $\frac{3}{2}^+$ isoanalog resonance state. The Erlangen group accordingly measured and

analyzed energy-averaged $\sigma(\theta)$, $\sigma P(\theta)$, and $\sigma A(\theta)$ data as a function of the scattering angle θ in the vicinity of each resonance, with P denoting the polarization and A representing the analyzing power. The results were compared with theoretical data obtained from FLIPPER computations performed with and without off-resonance DI contributions of type (a), and with and without off-resonance CN contributions of type (b).

The findings clearly demonstrated the presence of channel correlations, particularly in the data for the 6.81-MeV resonance. Lying below the 7-MeV (p,n) threshold and involving only a small DI admixture, the lowest of the three resonances offers the most conclusive evidence. In spite of its relatively small magnitude, the DI admixture nevertheless plays a crucial role in the channel correlations for CN decay, since it is responsible for the existence of interference terms in the energy-averaged fluctuating S matrix when the averaging embraces many fine-structure subresonances. Such correlations find no place in conventional Hauser-Feshbach theory, but are an intrinsic feature of the unified approach. An earlier indicant of this was evident in a study of similar data for the ^{92}Mo(p,p'_1) reaction: A simplified variant[13] of the Engelbrecht-Weidenmüller formalism[8] neglecting off-resonant CN absorption in resonant channels (i.e., a pure "doorway" treatment) was able to render a reasonable account of the observed differential cross section and polarization distributions as a function of the scattering angle.[24,25]

Contrasting with these proton scattering investigations for medium-mass nuclei, and more closely related to the present studies, is a set of analyses performed by Konshin[26] for neutron-induced reactions on the actinides, ^{242}Pu and ^{239}Pu. Apart from the results presented in paper I (see also Ref. 50), these explorations of the unified theory constitute the only other reported instances of quantitative evaluation. In these studies, too, a major simplification was introduced to enable the calculations to be performed: The unified formalism was employed in a restricted, purely statistical, form[10] excluding any DI contribution, and hence was incapable of providing information on possible channel-correlation interference. The energy dependence of the ^{242}Pu(n,f) fission cross section from $E_n=0.4$ to 1.2 MeV, as calculated along these restricted lines, provided a somewhat better fit to measured data than could be attained with conventional Hauser-Feshbach theory. However, the unified results systematically lay about 18% too high (whereas the Hauser-Feshbach cross sections were consistently 28% too high). This discrepancy vanished for Hauser-Feshbach-Moldauer calculations in which provision for the effect of level-width fluctuations was incorporated (causing a diminution of the inelastic cross section and an enhancement of the elastic one). No such option for the inclusion of width-fluctuation effects was contained in the unified computations. These and other analyses by Konshin involving fission channels demonstrated the importance of making allowance for $(n,\gamma f)$ contributions[27–31] in such calculations. For ^{239}Pu targets, analyses of (n,f), (n,γ), and (n,n') data were undertaken. The measured ^{239}Pu(n,f) data from $E_n \simeq 0.002$ to 0.6 MeV lay consistently lower than the calculated predictions; again, the closest fit ensued from Hauser-Feshbach-Moldauer theory with width-fluctuation corrections, while the unified cross sections exceeded the experimental data by approximately 15–20%, and the uncorrected Hauser-Feshbach predictions were roughly 30% too high. For ^{239}Pu(n,γ) radiative capture data, the unified results up to $E_n=0.7$ MeV matched the experimental values well, particularly at the higher energies, whereas the Hauser-Feshbach results lay about 15% too high (except in the region below $E_n \simeq 0.01$ MeV, where they were in close agreement).

Of particular interest for comparison with the present analyses was a set of five level excitation functions for ^{239}Pu(n,n') from threshold to $E_n=2$ MeV and a total (n,n') excitation function to 5 MeV. Unfortunately, the experimental error limits were rather large, particularly so in the case of the summed (n,n') data ($\pm 50\%$), detracting from the stringency of the theoretical comparisons. Within these uncertainties, the measured data tallied closely with the theoretical curves in the majority of instances; the author claimed that, when suitable allowance is made for fission competition, the calculated results do not effectively distinguish between the unified and the Hauser-Feshbach-Moldauer formalisms. Specifically, for scattering from the $\frac{1}{2}^+$ ground state in ^{239}Pu, a good match resulted for data referring to the 164-keV $(\frac{9}{2}^+)$ fifth member of the $\frac{1}{2}[631]$ ground-state rotational band, a fairly close match with those for the 286-keV $(\frac{5}{2}^+)$ lowest and 330-keV $(\frac{7}{2}^+)$ next-lowest members of the $\frac{5}{2}[622]$ band, and an excellent match with the combined data for the 388-keV state ($\frac{9}{2}^+$, third member of the $\frac{5}{2}[622]$ band) and the 392-keV state ($\frac{7}{2}^-$, lowest member of the $\frac{7}{2}[743]$ band). However, only fair agreement was obtained with the composite data for the 57-keV $(\frac{5}{2}^+)$ and 76-keV $(\frac{7}{2}^+)$ third

and fourth members of the $\frac{1}{2}[631]$ ground-state rotational band. For the summed (n,n') experimental data at $E_n=2$, 3, and 4 MeV, the CN calculations alone sufficed to provide a reasonable fit, but the addition of a DI contribution above $E_n=1$ MeV improved the quality of the fit still further and resulted in a smoother variation of the excitation function with incident energy. The author contended, in summary, that the unified approach was unreliable below about $E_n \simeq 1$ MeV, due to the relatively small number of open exit channels and to the strong fission competition, while thereafter the quantitative results from the various approaches tended to become indistinguishable from one another, although in essence the unified formalism was to be preferred. Already at 1.1 MeV the neutron cross sections for (n,γ), (n,f), and (n,n') processes for ^{242}Pu targets, respectively, agreed within 10%, 10%, and 2% in a comparison between Hauser-Feshbach-Moldauer theory and unified statistical theory. Only for elastic (n,n) data was there a noticeable difference at 1.2 MeV: The Hauser-Feshbach-Moldauer cross section was about three times as large as that calculated without width-fluctuation corrections, while the unified cross section was twice as large as the latter.

In the analyses of ^{232}Th(n,n') and ^{238}U(n,n') excitation functions for scattering to levels in vibrational bands, of which some preliminary results were illustrated in paper I and the rest are contained in the present paper (as also in Ref. 50), a collective coupled-channels treatment of direct channels was employed and no simplifying conditions were imposed upon the unified formalism. Hence the full basic resources of the unified approach were utilized. To assist in the identification of various influences amid the complexities of the intrinsic formalism, additional corrections and refinements were avoided, such as provision for radiative capture and fission competition, etc. These options, desirable in the case of fertile even-A actinide targets and essential to the treatment of fissile odd-A actinides, will be examined in more detail in a subsequent paper (paper III).

III. UNIFIED STATISTICAL S-MATRIX FORMALISM

In formal nuclear reaction theory, the most natural description of scattering employs the Heisenberg scattering matrix, defined through the asymptotic form of the quantal state function

$$\Psi_a \sim \mathscr{I}_a + \sum_b \mathscr{S}_{ab} \mathscr{O}_b \tag{2}$$

for the incident channel a, wherein $\mathscr{I}_a$ represents normalized incoming waves in channel a, and $\mathscr{O}_b$ the outgoing waves far from the scattering center in all open exit channels b. The S-matrix element S_{ab}, representing the probability amplitude for the transition from channel a to a particular exit channel b in the course of a scattering interaction, is a constituent of the grand-ensemble, symmetric (i.e., time-reversal invariant), unitary (flux-conserving) S matrix which embodies the physics of the process. Denoting energy averaging by the angle brackets $\langle \ldots \rangle$, one interprets the averaged diagonal elements $\langle S_{aa} \rangle$ as the elastic scattering amplitudes, with the channel label a containing the totality of quantum numbers, etc., that specify the system. The off-diagonal elements then denote the nonelastic, direct components. The energy averaging is, in practice, performed automatically in the calculations through the adoption of a complex optical potential containing an imaginary energy-dependent term W to describe the scattering interaction and absorption. In these circumstances, ancillary ensemble averaging becomes unnecessary, as was proved in subsidiary computations. The composite S matrix can be subdivided into components which vary only slightly with incident energy, and hence are effectively equal to their energy average over a reasonably small interval ΔE, and components which fluctuate strongly with energy, viz.,

$$S_{ab} = \langle S_{ab} \rangle + S_{ab}^{\mathrm{fl}} \, . \tag{3}$$

The former can be associated with direct processes; the latter constitute fluctuation amplitudes which ultimately yield a fluctuation cross section that corresponds to the "compound" mechanism, albeit coherent and hence qualitatively of different magnitude than the conventional Hauser-Feshbach σ_{CN}. This splitting of the S matrix can be theoretically justified (a) if the energy interval ΔE is significantly larger than the width Γ_{CN} and the separation D_{CN} of the CN resonances, and the fluctuations average out statistically to zero:

$$\Delta E \gg \Gamma_{\mathrm{CN}}, D_{\mathrm{CN}} \, ; \tag{4}$$

$$\langle S_{ab}^{\mathrm{fl}} \rangle = 0 \, , \tag{5}$$

and (b) if the energy interval ΔE is significantly smaller than the DI width Γ_{DI}, so that further energy averaging does not change the averaged component:

$$\Delta E \ll \Gamma_{\mathrm{DI}} \, ; \tag{6}$$

$$\langle \langle S_{ab} \rangle \rangle = \langle S_{ab} \rangle \, . \tag{7}$$

Under these conditions, the averaged second mo-

ments of the S matrix reduce from the form

$$\langle S_{ab}S_{cd}^{*}\rangle=\langle\langle S_{ab}\rangle\langle S_{cd}^{*}\rangle\rangle+\langle\langle S_{ab}\rangle S_{cd}^{\mathrm{fl}*}\rangle+\langle\langle S_{ab}^{*}\rangle S_{cd}^{\mathrm{fl}}\rangle+\langle S_{ab}^{\mathrm{fl}}S_{cd}^{\mathrm{fl}*}\rangle \tag{8}$$

to

$$\langle S_{ab}S_{cd}^{*}\rangle=\langle S_{ab}\rangle\langle S_{cd}^{*}\rangle+\langle S_{ab}^{\mathrm{fl}}S_{cd}^{\mathrm{fl}*}\rangle\ , \tag{9}$$

where the asterisk denotes complex conjugation and the double angular brackets signify double energy averaging. In this reduction, the vanishing of the interference cross terms in Eq. (8) as a consequence of the conditions (7) and (5) provides the justification for separating the fluctuating and direct components of the S matrix in Eq. (3) and excluding any interference between these elements. Thus, in the spirit of the Hauser-Feshbach theory,[32] one obtains an integrated cross section for a single compound state (in units of $\pi\lambda^2$, and omitting geometrical vector-addition and kinematical factors) as

$$\sigma_{ab}=|\,\delta_{ab}-S_{ab}\,|^2=\langle\sigma_{ab}^{\mathrm{fl}}\rangle+\sigma_{ab}^{\mathrm{DI}}\ , \tag{10}$$

in which

$$\langle\sigma_{ab}^{\mathrm{fl}}\rangle=\langle\,|\,S_{ab}^{\mathrm{fl}}\,|^2\rangle \tag{11}$$

and

$$\sigma_{ab}^{\mathrm{DI}}=|\,\delta_{ab}-\langle S_{ab}\rangle\,|^2=|\,\delta_{ab}-S_{ab}-S_{ab}^{\mathrm{fl}}\,|^2\ , \tag{12}$$

wherein δ_{ab} constitutes a Kronecker δ symbol for the incoming channel a and outgoing channel b. The unitarity of $\mathscr{S}$, expressing probability conservation, viz.,

$$(\mathscr{S}\mathscr{S}\dagger)_{ab}=\sum_c\mathscr{S}_{ac}\mathscr{S}_{bc}^{*}=\delta_{ab}\ , \tag{13}$$

leads to a definition of transmission coefficients in the absence of direct reactions,

$$T_a=1-|\,\langle S_{aa}\rangle\,|^2\ , \tag{14}$$

expressing the probability of compound nucleus formation in channel a, and thence leading to a Hauser-Feshbach penetrability term for the $a\to b$ transition sequence:

$$\tau\equiv T_aT_b/\sum_c T_c\ . \tag{15}$$

In the presence of direct reactions this becomes generalized. The unitarity deficit of the averaged S matrix is expressed[33] through generalized transmission coefficients T_{ab},

$$T_{ab}=\sum_c\langle S_{ac}^{\mathrm{fl}}S_{cb}^{\mathrm{fl}*}\rangle\equiv\delta_{ab}-\sum_c\langle S_{ac}\rangle\langle S_{cb}^{*}\rangle\ , \tag{16}$$

which are elements of the Satchler penetrability matrix[33] $\mathscr{P}$. Then, if $\langle\mathscr{S}\rangle$ is diagonal, the generalized coefficients reduce to the conventional transmission coefficients via the relation $T_{ab}\to\delta_{ab}T_a$, and the formalism reverts to expression (14). Since the $\mathscr{S}$ matrix is symmetric, the $\mathscr{P}$ matrix is Hermitian, and can be diagonalized through a unitary transformation which lies at the root of the Engelbrecht-Weidenmüller approach[8]:

$$(\mathscr{U}\mathscr{P}\mathscr{U}^{\dagger})_{ab}=\delta_{ab}p_a\ . \tag{17}$$

Through the extension of the formalism to include direct processes, one thus obtains inherently "generalized transmission coefficients" p_a; in the absence of DI these revert to T_a. The unitary transformation matrix $\mathscr{U}$ thus defined can be used to obtain a symmetric and unitary modified scattering matrix $\tilde{\mathscr{S}}$ as

$$\tilde{\mathscr{S}}=\mathscr{U}\mathscr{S}\mathscr{U}^{T}\ (\mathscr{U}^{T}=\text{ transposed }\mathscr{U}\text{ matrix})\ , \tag{18}$$

whose energy average is a diagonal matrix (since $\mathscr{U}\langle\mathscr{S}\rangle\mathscr{U}^{T}$ is diagonal):

$$\langle\tilde{\mathscr{S}}\rangle=\delta_{ab}\langle\tilde{S}_{ab}\rangle\ . \tag{19}$$

One then obtains the relation between energy-averaged second moments as

$$\langle S_{ab}^{\mathrm{fl}}S_{cd}^{\mathrm{fl}*}\rangle=\sum_{efgh}U_{ea}^{*}U_{fb}^{*}U_{gc}U_{hd}\langle\tilde{S}_{ef}^{\mathrm{fl}}\tilde{S}_{gh}^{\mathrm{fl}*}\rangle\ . \tag{20}$$

In the restricted theory devoid of DI, such terms as $\langle S_{ab}^{\mathrm{fl}}S_{cd}^{\mathrm{fl}*}\rangle$ can be calculated in terms of $\langle S_{ef}\rangle$ and, aside from a trivial phase factor, depend simply on the transmission coefficients T_a; they vanish whenever one of the four indices a,b,c,d differs from the other three, leaving only $\langle\,|\,S_{ab}^{\mathrm{fl}}\,|^2\rangle$ and $\langle S_{aa}^{\mathrm{fl}}S_{bb}^{\mathrm{fl}*}\rangle$ as nonzero terms. The latter can be parametrized, using an approximation formula[10] (which was found to give the same results as the later variant in Ref. 12) for the "elastic enhancement factor,"

$$W_a=1+\frac{2}{1+p_a^{0.3+1.5\psi}}+2\left[\psi-\frac{\bar{p}}{\sum_c p_c}\right]^2\ , \tag{21}$$

with the abbreviation $\psi\equiv p_a/\sum_c p_c$, and $\bar{p}$ the arithmetic mean of all the p_a (wherein $p_a=T_a$ throughout in this simple situation). The values of W_a vary from about 3 for weak absorption to about 2 for strong absorption in all channels. The gen-

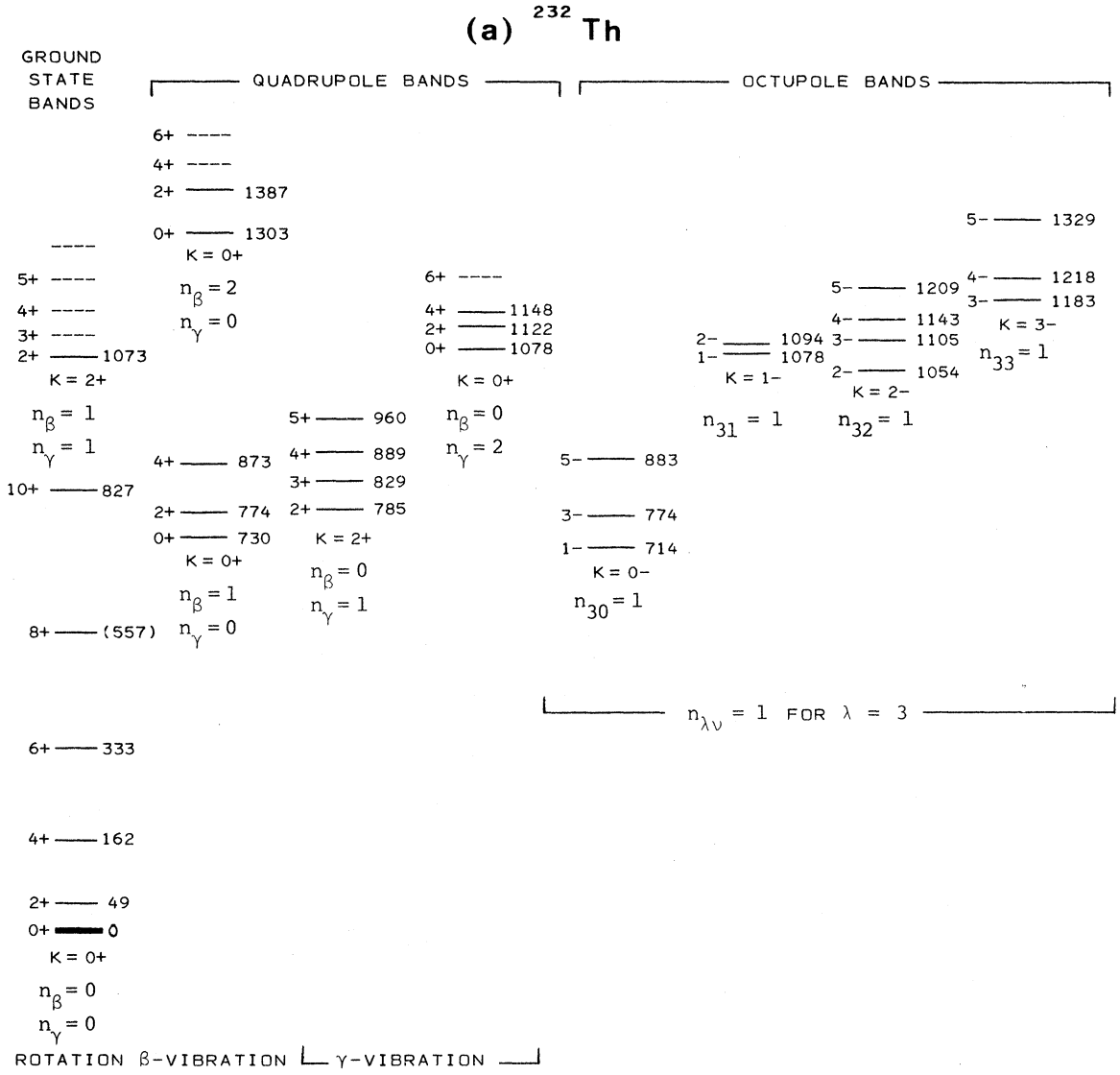

FIG. 1. Decomposition of the collective (rotational and vibrational) band level schemes of (a) ^{232}Th and (b) ^{238}U, with level energies cited as in Nuclear Data Sheets (differing slightly from those adopted by the Lowell group in paper I and the present paper).

eralized transmission coefficients are expressible in terms of these quantities and V parameters as

$$p_a \equiv \sum_b \langle |S_{ab}^{\rm fl}|^2 \rangle = V_a + (W_a - 1)V_a^2 / \sum_c V_c \ . \quad (22)$$

Instead of solving this unitarity relation directly to obtain the V_a, Hofmann *et al.*[10] replaced the one-step iteration treatment that had been used earlier by a two-step procedure that gave the result

$$V_a = p_a[1 + (W_a - 1)V_a^{(1)} / \sum_c V_c^{(1)}]^{-1} \quad (23)$$

with

$$V_a^{(1)} \equiv p_a[1 + (W_a - 1)\psi]^{-1} \ . \quad (24)$$

Then, akin to Eq. (15), one finds

$$\langle |\tilde{S}_{ab}^{\rm fl}|^2 \rangle = V_a V_b / \sum_c V_c \quad (\text{if } a \neq b) \quad (25)$$

and (if $a = b$)

$$\langle |\tilde{S}_{aa}^{\rm fl}|^2 \rangle = W_a V_a^2 / \sum_c V_c \ . \quad (26)$$

In the absence of direct reactions one may set $\tilde{\mathcal{S}} = \mathcal{S}$ in the derivation of interaction cross sections, using Eq. (26) and the following expression (27) for $\langle S_{aa}^{\rm fl} S_{bb}^{\rm fl*} \rangle$:

$$\langle \tilde{S}_{aa}^{\rm fl} \tilde{S}_{bb}^{\rm fl*} \rangle = e^{2i(\phi_a - \phi_b)} X_a X_b \ , \quad (27)$$

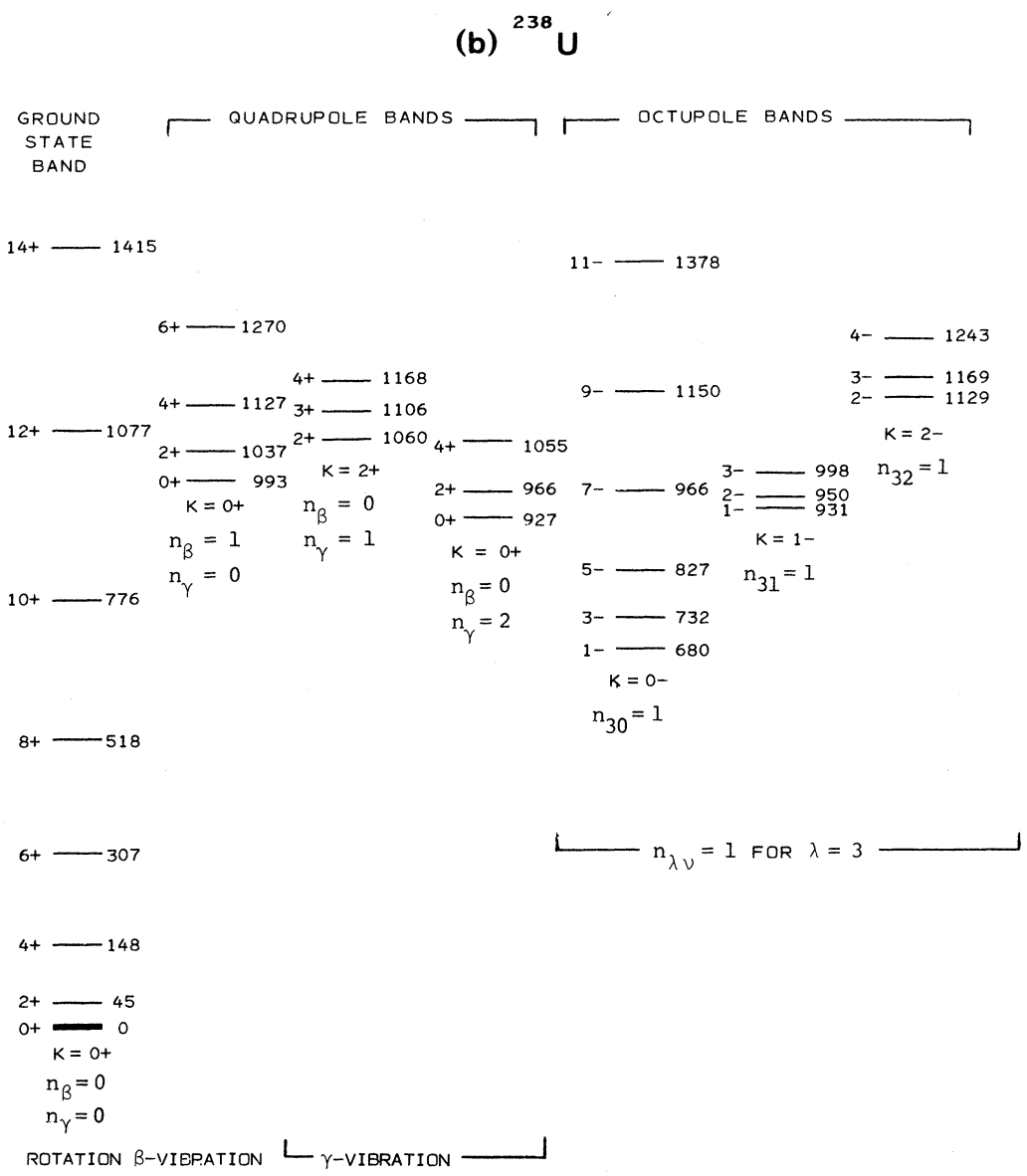

FIG. 1. (*Continued.*)

once again making the identification $\tilde{\mathscr{S}} = \mathscr{S}$. Formula (27) ensues from the Engelbrecht-Weidenmüller approach[8] in which a phase ϕ is introduced through the relation

$$\langle \tilde{S}_{aa} \rangle = e^{2i\phi_a}(1-p_a)^{1/2} , \tag{28}$$

such that

$$\langle \tilde{S}^{\mathrm{fl}}_{aa} \tilde{S}^{\mathrm{fl}*}_{bb} \rangle e^{-2i(\phi_a - \phi_b)}$$

is real and positive. Then, in terms of parameters X_a, where

$$X_a = Y_a(1 - Y_a + 4Y_a^2) , \tag{29}$$

with

$$Y_a \equiv \left[\frac{V_a^2}{\sum_c V_c} \right]^{1/2} \frac{(1-p_a)^{1/2}}{1+0.15\sum_c p_c} , \tag{30}$$

one obtains the result (27).

However, in the presence of direct reactions, one has to determine the elements T_{ab} of the transmission matrix as in Eq. (16), and thence calculate the

TABLE I. ^{232}Th(n,n') angle-integrated cross sections (in mb) for inelastic neutron scattering from 0.8 to 2.5 MeV, computed with CINDY, KARJUP, and NANCY, using the Haouat-Lagrange (Bruyères) optical potential and deformation parameters.

Level energy E^* (keV)	Level spin J^π	Collective band identification K^π Character	Theoretical formalism	Coupling strength admixture	$\sigma(n,n')$ in mb at incident neutron energy 0.8	1.0	1.2 MeV	1.5	2.0	2.5
714.3	1^-	0^- octupole	Standard CN		145.6	206.5	168.4	109.0	60.2	46.3
			Standard DI	0.30		49.2	78.0	123.5	195.8	232.1
			CN + DI			255.7	246.4	232.5	256.0	278.4
			Unified	0.30	244.4	386.6	338.9	261.4	235.3	219.2
730.4	0^+	0^+ β vibration	Standard CN		44.0	71.9	60.4	39.4	20.7	16.1
			Standard DI	0.02		0.8	1.5	3.5	9.3	15.6
			CN + DI			72.7	61.9	42.9	30.0	31.7
			Unified	0.01	78.0	140.1	118.7	80.5	67.5	57.2
774.1	2^+	0^+ β vibration	Standard CN		40.2	148.1	144.7	109.7	72.5	59.9
			Standard DI	0.02		2.0	4.1	9.2	10.1	12.7
			CN + DI			150.1	148.8	118.9	82.6	72.6
			Unified	0.10	73.6	276.5	282.1	251.1	257.3	259.0
774.4	3^-	0^- octupole	Standard CN		25.2	104.0	114.2	95.4	72.6	62.4
			Standard DI	0.30		19.2	28.2	37.6	52.1	93.6
			CN + DI			123.2	140.6	133.0	124.7	156.0
			Unified	0.30	54.1	271.5	266.3	235.6	239.5	237.6
774 combined	2^+,		Standard CN	(summed)	65.4	252.1	257.1	205.1	145.1	122.3
	3^-		Standard DI	0.02,0.30		21.1	32.2	46.8	62.2	106.3
			CN + DI	(summed)		273.2	289.3	251.9	207.3	228.6
			Unified	0.10,0.30	127.7	548.0	548.4	486.7	496.8	496.6
785.2	2^+	2^+ γ vibration	Standard CN		23.7	136.0	138.2	107.6	71.8	59.5
			Standard DI	0.12		113.9	144.3	194.3	260.9	296.5
			CN + DI			249.9	282.5	301.9	332.7	329.0
			Unified	0.08		300.2	311.6	276.3	282.6	288.4
829.6	3^+	2^+ γ vibration	Standard CN			77.7	98.2	89.7	69.9	60.9
			Standard DI	0.12		7.2	12.9	15.0	14.2	15.2
			CN + DI			84.9	111.1	104.7	84.1	76.1
			Unified	0.08		135.2	173.4	165.5	182.2	188.7
873.0	4^+	0^+ β vibration	Standard CN			37.6	55.5	56.3	50.5	48.0
			Standard DI	0.02		0.2	0.7	2.7	6.7	8.1
			CN + DI			37.8	56.2	59.0	57.2	56.1
			Unified	0.01		46.2	81.2	100.5	128.0	135.7
883.3	5^-	0^- octupole	Standard CN			2.3	10.1	18.9	26.2	30.2
			Standard DI	0.30		0.0	0.5	5.0	34.6	59.2
			CN + DI			2.3	10.6	23.9	60.8	89.4
			Unified	0.10		6.9	16.2	30.9	57.8	70.5
890.1	4^+	2^+ γ vibration	Standard CN			34.0	54.9	56.4	50.4	47.9
			Standard DI	0.12		0.7	3.0	7.2	20.2	46.8
			CN + DI			34.7	57.9	63.6	70.6	94.7
			Unified	0.08		36.2	82.9	108.1	151.0	161.6
960.2	5^+	2^+ γ vibration	Standard CN			0.5	6.5	16.1	24.4	29.1
			Standard DI	0.12			0.0	0.1	1.1	1.8
			CN + DI				6.5	16.2	25.5	30.9
			Unified	0.08		5.9	35.3	49.2	81.5	99.9

generalized transmission coefficients p_a in accordance with Eq. (17), using computational procedures for matrix diagonalization which furnish the elements of the $\mathscr{U}$ matrix needed for the transformations (20). The terms $\langle |\tilde{S}_{ab}^{\mathrm{fl}}|^2 \rangle$ can be calculated as in Eq. (25) and the parameters ϕ_a and X_a computed from Eqs. (28)—(30). Then the averaged product (27) can be evaluated, together with

TABLE I. (*Continued.*)

Level energy E^* (keV)	Level spin J^π	Collective band identification K^π	Character	Theoretical formalism	Coupling strength admixture	$\sigma(n,n')$ in mb at incident neutron energy 0.8 MeV	1.0 MeV	1.2 MeV	1.5 MeV	2.0 MeV	2.5 MeV
1053.6	2^-	2^-	octupole	Standard CN				53.8	73.4	59.1	52.0
				Standard DI	0.10			4.6	8.1	7.6	7.3
				CN + DI				58.4	81.5	66.7	59.3
				Unified	0.01			111.3	122.5	112.7	108.9
1077.5	1^-	1^-	octupole	Standard CN				51.1	66.9	46.7	39.3
				Standard DI	0.10			20.3	52.6	72.1	70.8
				CN + DI				71.4	119.5	118.8	110.1
				Unified	0.01			105.6	131.5	106.2	91.6
1078.7	0^+	0^+	γ vibration	Standard CN				20.0	25.5	16.7	13.8
				Standard DI	0.10			9.5	23.9	18.3	22.2
				CN + DI				29.5	49.4	35.0	36.0
				Unified				51.4	74.4	61.5	56.1
1094.4	2^-	1^-	octupole	Standard CN				40.2	68.1	57.4	51.7
				Standard DI	0.10			5.2	12.5	15.4	28.2
				CN + DI				45.4	80.6	72.8	79.9
				Unified	0.01			82.9	132.5	125.2	120.8
1105.7	3^-	2^-	octupole	Standard CN				33.6	60.3	57.0	53.9
				Standard DI	0.10			3.8	13.9	12.6	15.0
				CN + DI				37.4	74.2	69.6	68.9
				Unified	0.01			51.8	96.8	108.8	119.5
1122.8	2^+	0^+	γ vibration	Standard CN				30.5	64.5	56.5	51.4
				Standard DI	0.10			2.5	21.8	34.1	74.0
				CN + DI				33.0	86.3	90.6	125.4
				Unified				81.0	228.8	205.2	187.5
1143.3	4^-	2^-	octupole	Standard CN				16.5	36.7	39.8	42.1
				Standard DI	0.10			0.7	0.4	1.8	6.1
				CN + DI				17.2	37.1	41.6	48.2
				Unified	0.01			15.8	49.6	75.3	96.1
1147.9	4^+	0^+	γ vibration	Standard CN				15.6	37.5	54.3	42.7
				Standard DI	0.10			0.5	9.0	31.9	44.6
				CN + DI				16.1	46.5	86.2	87.3
				Unified				20.7	132.1	147.4	160.0
1182.5	3^-	3^-	octupole	Standard CN					53.6	55.1	53.4
				Standard DI	0.10				47.3	95.2	87.9
				CN + DI					100.9	150.3	141.3
				Unified	0.01			6.2	86.4	105.8	116.1
1208.9	5^-	2^-	octupole	Standard CN					6.6	17.5	24.9
				Standard DI	0.10				0.0	2.1	5.4
				CN + DI					6.6	19.6	30.3
				Unified	0.01				10.0	34.5	57.7
1218.1	4^-	3^-	octupole	Standard CN					31.7	37.7	41.0
				Standard DI	0.10				0.1	0.5	2.6
				CN + DI					31.8	38.1	46.3
				Unified	0.01				45.4	69.5	88.2

$$\langle S_{ab}^{\mathrm{fl}} S_{cd}^{\mathrm{fl}*} \rangle = \sum_{e,f} (1-\delta_{ef}) [U_{ea}^* U_{fb}^* (U_{ec} U_{fd} + U_{fc} U_{ed}) \langle |\tilde{S}_{ef}^{\mathrm{fl}}|^2 \rangle + U_{ea}^* U_{eb}^* U_{fc} U_{fd} \langle \tilde{S}_{ee}^{\mathrm{fl}} \tilde{S}_{ff}^{\mathrm{fl}*} \rangle] + \sum_{e} U_{ea}^* U_{eb}^* U_{ec} U_{ed} \langle |\tilde{S}_{ee}^{\mathrm{fl}}|^2 \rangle , \tag{31}$$

TABLE II. $^{238}U(n,n')$ angle-integrated cross sections (in mb) for inelastic neutron scattering from 0.8 to 2.5 MeV, computed with CINDY, KARJUP, and NANCY, using the Haouat-Lagrange (Bruyères) optical potential and deformation parameters

Level energy E^* (keV)	Level spin J^π	Collective band identification K^π	Character	Theoretical formalism	Coupling strength admixture	$\sigma(n,n')$ in mb at incident neutron energy 0.8	1.0	1.2	1.5 MeV	1.6	2.0	2.5
680.0	1^-	0^-	octupole	Standard CN		228.8	255.4	156.8		95.2	71.0	56.4
				Standard DI	0.42		110.7	145.4		200.9	259.7	288.7
				CN + DI			366.1	302.2		296.1	330.7	345.1
				Unified	0.32	266.2	356.0	278.1	234.0		226.3	218.9
731.9	3^-	0^-	octupole	Standard CN		80.7	166.3	123.8		94.1	81.9	73.6
				Standard DI	0.42		11.5	25.4		59.6	120.6	187.0
				CN + DI			177.8	149.0		153.7	202.5	260.6
				Unified	0.30	126.0	266.9	245.5	224.5		233.3	239.1
827.2	5^-	0^-	octupole	Standard CN			6.4	13.3		22.8	29.6	35.6
				Standard DI	0.42		0.1	0.9		11.1	36.3	49.6
				CN + DI			7.5	14.2		33.9	65.9	85.2
				Unified	0.01		9.4	19.1	29.5		48.8	60.1
927.2	0^+	0^+	γ vibration	Standard CN			29.2	38.8		29.3	22.7	18.9
				Standard DI	0.06			10.6		13.8	10.8	8.7
				CN + DI				49.4		43.1	33.5	27.6
				Unified			78.9	132.1	93.4		74.1	58.2
930.8	1^-	1^-	octupole	Standard CN			75.1	103.1		77.5	61.4	51.5
				Standard DI	0.10			41.9		62.4	66.1	77.3
				CN + DI				145.0		139.9	127.5	128.8
				Unified	0.15		136.9	209.4	155.9		134.5	127.3
950.0	2^-	1^-	octupole	Standard CN			49.8	98.1		84.7	73.6	66.6
				Standard DI	0.10			11.2		12.2	21.6	42.9
				CN + DI				109.3		96.9	95.2	109.5
				Unified	0.10		80.8	181.6	138.1		122.1	113.0
966.3	2^+	0^+	γ vibration	Standard CN			33.3	89.7		82.4	72.5	65.9
				Standard DI	0.06			9.5		18.8	37.7	36.3
				CN + DI				99.2		101.2	110.2	102.2
				Unified			69.4	365.4	306.0		244.3	198.8
993.0	0^+	0^+	β vibration	Standard CN				30.5		27.3	21.7	18.3
				Standard DI	0.05			9.4		33.2	68.5	97.9
				CN + DI				39.9		60.5	90.2	116.2
				Unified	0.01			78.4	66.3		56.7	51.0
997.5	3^-	1^-	octupole	Standard CN				63.7		68.0	66.2	65.1
				Standard DI	0.10			51.1		63.8	62.3	63.0
				CN + DI				114.8		131.8	128.5	128.1
				Unified	0.10			133.2	126.7		139.1	142.5
1037.3	2^+	0^+	β vibration	Standard CN				64.6		76.4	69.3	64.2
				Standard DI	0.05			13.2		26.7	40.2	52.0
				CN + DI				77.8		103.1	109.5	116.2
				Unified	0.01			134.6	150.6		147.3	138.7
1055.0	4^+	0^+	γ vibration	Standard CN				30.2		40.3	44.8	49.7
				Standard DI	0.06			1.8		7.5	12.6	24.8
				CN + DI				32.0		47.8	57.4	74.5
				Unified				132.4	177.0		173.8	168.1

where the summations proceed over all open channels e, f, including the elastic channel ($e=f$).

Thus, in contrast to conventional Hauser-Feshbach theory, in which one has

$$\langle S_{ab}^{\mathrm{fl}} S_{cd}^{\mathrm{fl}*} \rangle = \delta_{ac}\delta_{bd} \langle |S_{ab}^{\mathrm{fl}}|^2 \rangle , \tag{32}$$

the unified theory contains nonvanishing terms when $a \neq c$ and $b \neq d$ in the presence of DI in the

TABLE II. (*Continued.*)

Level energy E^* (keV)	Level spin J^π	Collective band identification K^π	Character	Theoretical formalism	Coupling strength admixture	$\sigma(n,n')$ in mb at incident neutron energy 0.8	1.0	1.2	1.5 MeV	1.6	2.0	2.5
1060.9	2^+	2^+	γ vibration	Standard CN				56.9		76.2	69.8	64.8
				Standard DI	0.50			18.7		57.1	80.5	115.3
				CN + DI				75.5		133.3	150.3	180.1
				Unified	0.01			109.7	131.9		136.0	133.5
1105.3	3^+	2^+	γ vibration	Standard CN				35.7		63.5	64.0	64.2
				Standard DI	0.50			0.8		6.0	10.1	13.0
				CN + DI				36.5		69.5	74.1	77.2
				Unified	0.10			61.8	127.0		148.9	159.9
1127.0	4^+	0^+	β vibration	Standard CN				18.9		39.1	44.0	49.5
				Standard DI	0.05			0.3		5.6	13.3	25.3
				CN + DI				19.2		44.7	57.3	74.8
				Unified				30.1	87.4		120.4	135.9
1128.9	2^-	2^-	octupole	Standard CN				31.5		71.1	67.9	64.4
				Standard DI	0.10			11.5		25.6	21.7	20.7
				CN + DI				43.0		96.7	89.6	85.1
				Unified	0.01			53.5	94.4		95.6	96.4
1167.4	4^+	2^+	γ vibration	Standard CN				10.7		37.8	43.1	49.2
				Standard DI	0.50					6.6	23.6	36.6
				CN + DI						44.4	66.7	85.8
				Unified				7.8	77.5		115.1	134.3
1169.4	3^-	2^-	octupole	Standard CN				15.3		60.8	62.8	64.2
				Standard DI	0.10			5.8		36.8	25.7	21.6
				CN + DI				21.1		97.6	88.5	85.8
				Unified	0.01			14.1	79.0		92.8	104.8
1243	4^-	2^-	octupole	Standard CN						33.1	40.1	47.6
				Standard DI	0.10					0.2	1.1	2.6
				CN + DI						33.3	41.2	50.2
				Unified	0.01				38.3		61.5	81.8
1269.4	6^+	0^+	β vibration	Standard CN						3.3	7.8	14.2
				Standard DI	0.05					0.1	0.1	0.1
				CN + DI						3.4	7.9	14.3
				Unified					2.3		19.4	38.6

respective channels. These nonvanishing interference terms have the same connotation as in the concept of channel correlation; from an explicit knowledge of their values one can calculate the phase-corrected fluctuation cross section and then build the total cross section through addition of the DI component in accordance with Eq. (10). Differential cross sections, polarization distributions, analyzing power, etc., can also be calculated, following the methods of Kawai *et al.*[34] An alternative approach to statistical nuclear reaction theory based upon entropy considerations has been developed by Mello and Seligman[35–39] in which several of the above features have been examined within the context of the S-matrix formalism. Though it has yielded good results in the case of strong absorption, its extension to the general domain of weaker absorption is still in the process of being refined. For our purposes, at this stage, the unified formulation as indicated in the foregoing appears to offer the most inviting and conclusive prospects.

IV. UNIFIED CALCULATIONS AND RESULTS

The essence of the unified approach lies in the coupling of transition channels coherently within a grand ensemble. In applying it to actinide target nuclei, which evince considerable deformation [see data below Eq. (1)] and a strongly collective character, the use of a coupled-channels DI computer program such as JUPITOR[5] is manifestly appropriate. The requisite unified program NANCY[4] has therefore been assembled in FORTRAN, modifying the subroutines of JUPITOR to generate the full aggregate of S-matrix elements from computed normal-

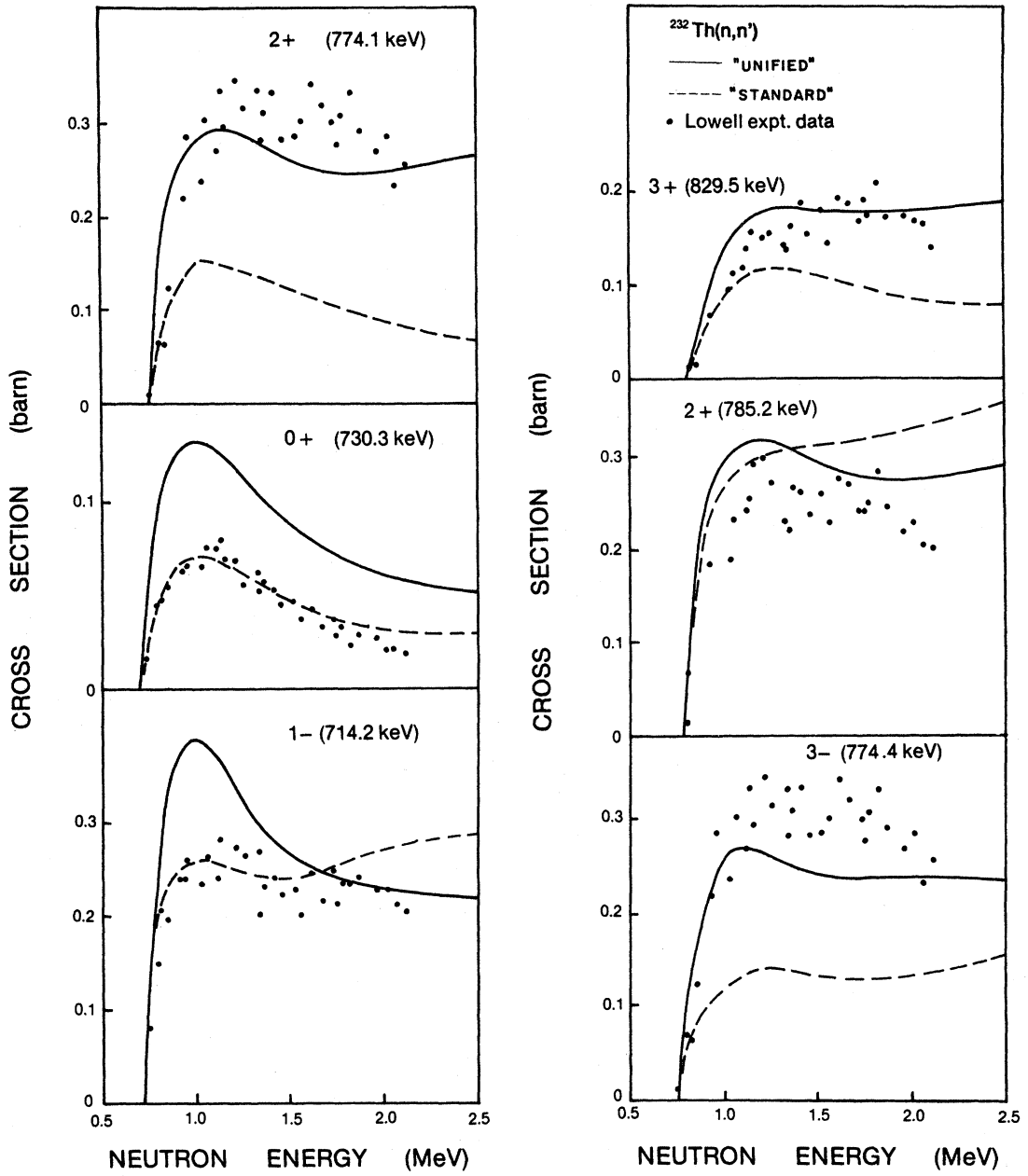

FIG. 2. Theoretical and experimental excitation functions for ^{232}Th(n,n') inelastic scattering to levels between 714.2 and 829.5 keV excitation energy (members of the $K=0^-$ octupole, $K=0^+$ β-vibrational, and $K=2^+$ γ-vibrational quadrupole bands). Experimental data (dots; the error limits are indicated in corresponding diagrams in paper I) are contrasted with theoretical unified (solid) curves and with the predictions of the standard (CN + DI) approach (broken curves), obtained from coupled-channel calculations. The numerical computed data are listed in Table I.

ized complex C-matrix elements via the transformation

$$S_{ab}=\delta_{ab}+2iC_{ab}\ , \tag{33}$$

coupling each state to every other (which entailed extending the coupling modes within JUPITOR, since in that program only the ground state is coupled in turn with each excited state: There are no intercouplings among the latter). For the derivation of matrix elements and transmission coefficients relating to the competition channels, the SCAT routine[40] was incorporated, thus providing additional diagonal elements, for which the energy averaging had already intrinsically been performed through the use

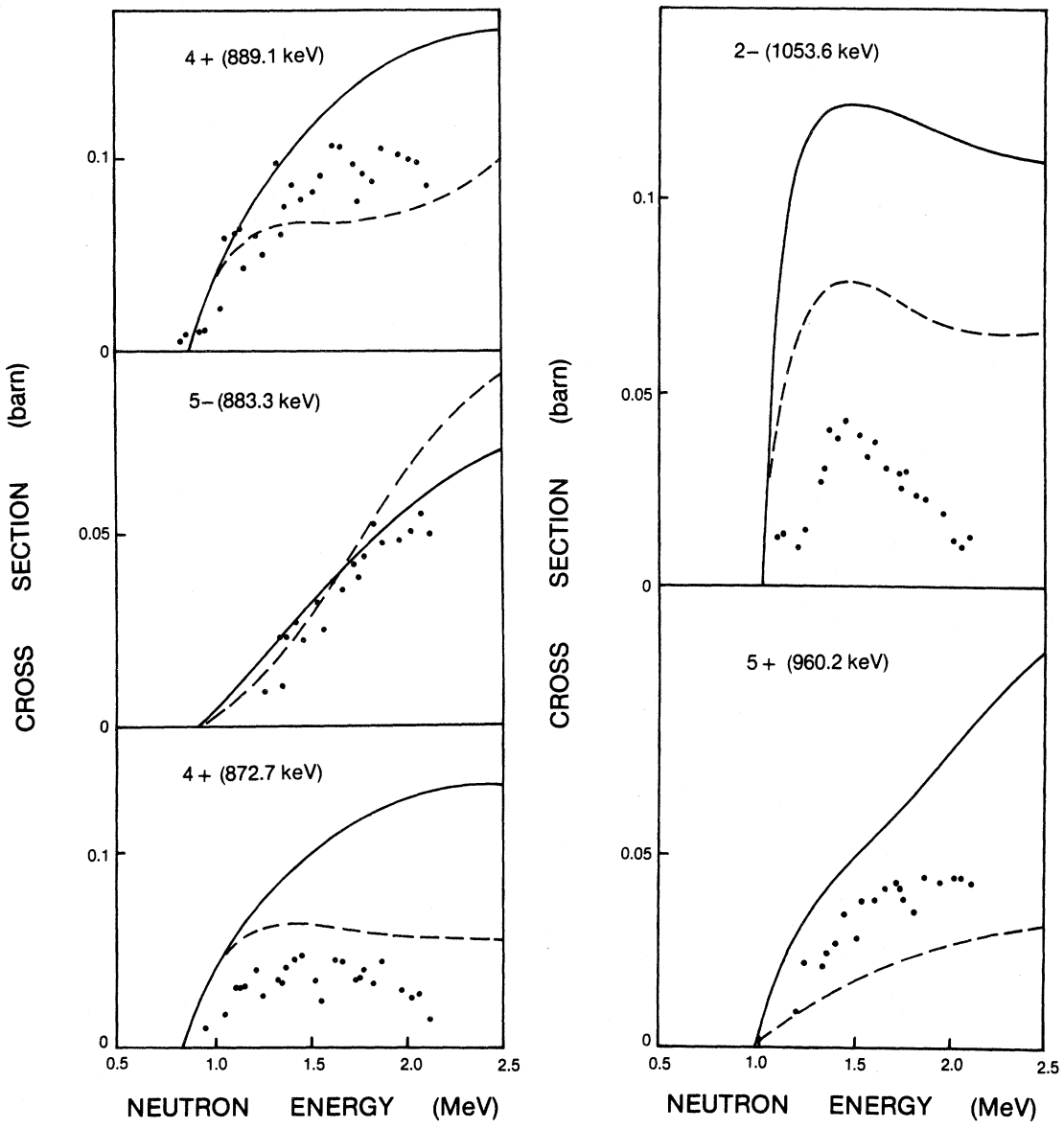

FIG. 3. Same as Fig. 2, but for ^{232}Th levels between 872.7 and 1053.6 keV that are members of the $K=0^+$ β-vibrational, 0^- octupole, 2^+ γ-vibrational, and 2^- octupole bands.

of a complex Woods-Saxon derivative optical potential with the Bruyères parameters cited in Eq. (1).

The computations were thus designed to be as consistent as possible with the methods adopted in paper I, retaining the same optical potential and deformation parameters, and the same SCAT routine as had been used in the statistical code CINDY[4] in paper I in the course of calculating CN cross sections. For the determination of DI cross sections and matrix elements, the JUPITOR program's procedures in NANCY were equivalent to those employed in KARJUP[6] (the Karlsruhe variant of JUPITOR) previously. The same energy-level schemes for the nuclei ^{232}Th and ^{238}U, separated into the same collective rotational and vibrational bands, and reproduced in Figs. 1(a) and (b), were adopted.

In NANCY, the precalculation of competing-channel penetrabilities enabled these to be used for computing the parameters V_a, $V_a^{(1)}$, W_a, X_a, Y_a, and the penetrability denominators $\sum_c p_c$ and $\sum_c V_c$. For the diagonalization of the $\mathscr{P}$ matrix, Householder's method[41] was utilized as a fast and accurate eigenvalue routine that furnished the requisite $\mathscr{U}$-matrix elements for use in the

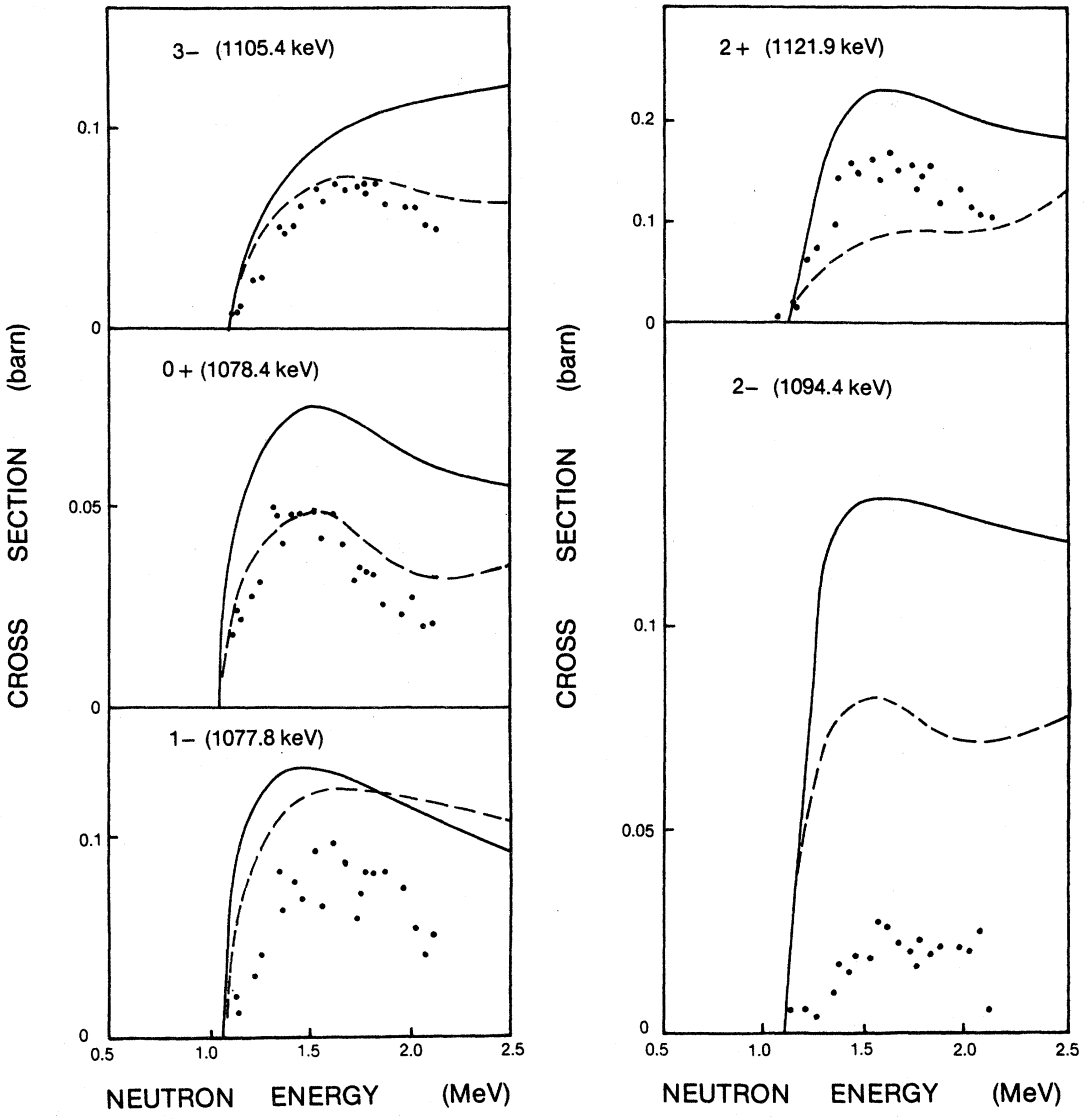

FIG. 4. Same as Fig. 2, but for ^{232}Th levels between 1077.8 and 1121.9 keV that are members of the $K=1^-$ octupole, 0^+ γ-vibrational, and 2^- octupole bands.

Engelbrecht-Weidenmüller transformation and other unitary transformations. Labeling the elements according to their channel number n, orbital momentum l, and total angular momentum j, (where unprimed quantities refer to the incoming channel and primed quantities to the outgoing channels), one obtains the energy-averaged integrated cross section explicitly as[42]

$$\langle \sigma_{nn'} \rangle = \pi \lambda\!\!\!^{-}_n{}^2 \sum g_J \{ | \delta_{ll'}\delta_{jj'} - \langle S^{J\pi}_{nlj;n'l'j'} \rangle |^2 + \langle | S^{J\pi}_{nlj;n'l'j'} |^2 \rangle \} , \tag{34}$$

incorporating the nuclear g factor

$$g_J \equiv \frac{2J+1}{(2I_n+1)(2s+1)} . \tag{35}$$

The summation in Eq. (34) is extended over all J, π, n, l, j, n', l', and j', with J^π representing the spin and parity of the intermediate state populated by the capture of a projectile having angular momentum $\vec{j} = \vec{l} + \vec{s}$ that impinged on a target nucleus of spin I_n in the nth state. To conserve core storage

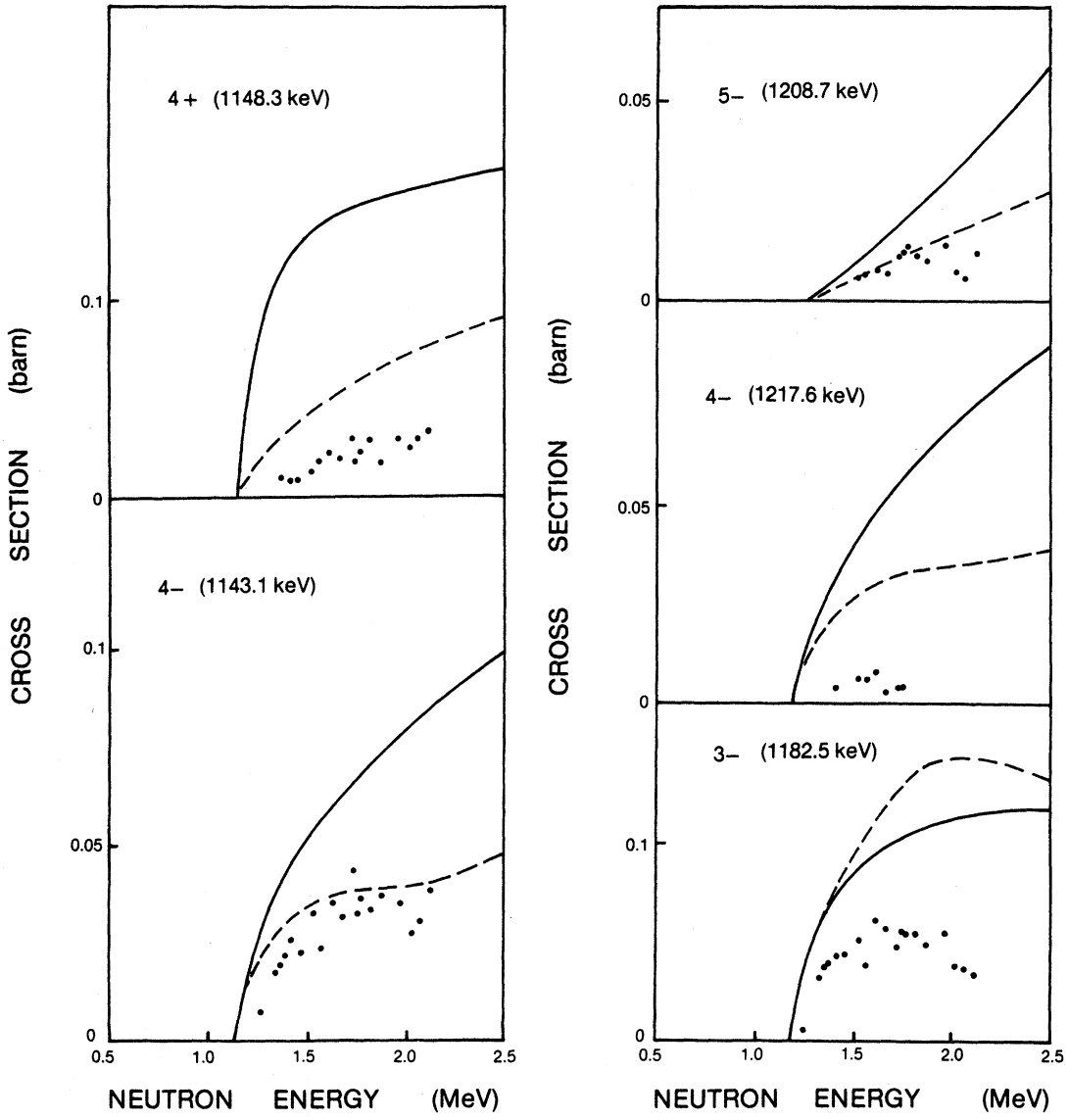

FIG. 5. Same as Fig. 2, but for ^{232}Th levels between 1143.1 and 1217.6 keV that are members of the $K=2^-$ octupole, 0^+ γ-vibrational, and 3^- octupole bands.

space, the direct S-matrix files were stored as record files (in disk storage) for later retrieval; the core memory storage requirement for NANCY in its unembellished form ran to 65 K words on a CDC Cyber-71 computer having 64-bit word capability.

The numerical results are listed in Tables I and II for ^{232}Th(n,n') and ^{238}U(n,n') scattering excitation functions, respectively. These tables also cite the CN, DI, and combined cross sections obtained from the standard (incoherent CN + DI) approach, as plotted in paper I, for comparison. Graphical representations of these data, compared with the experimental data of the Lowell group,[43,44,50] are presented in Figs. 2—5 for ^{232}Th levels and in Figs. 6—9 for ^{238}U levels.

V. DISCUSSION

In Fig. 2, the results for the 774.1-keV (2^+) level in ^{232}Th and the 774.4-keV (3^-) state have been depicted separately (although the "combined" measured data are the same, since the energies are too close to be experimentally resolvable). In all the analyses, the relative band coupling strength has been the only parameter to be adjusted for the at-

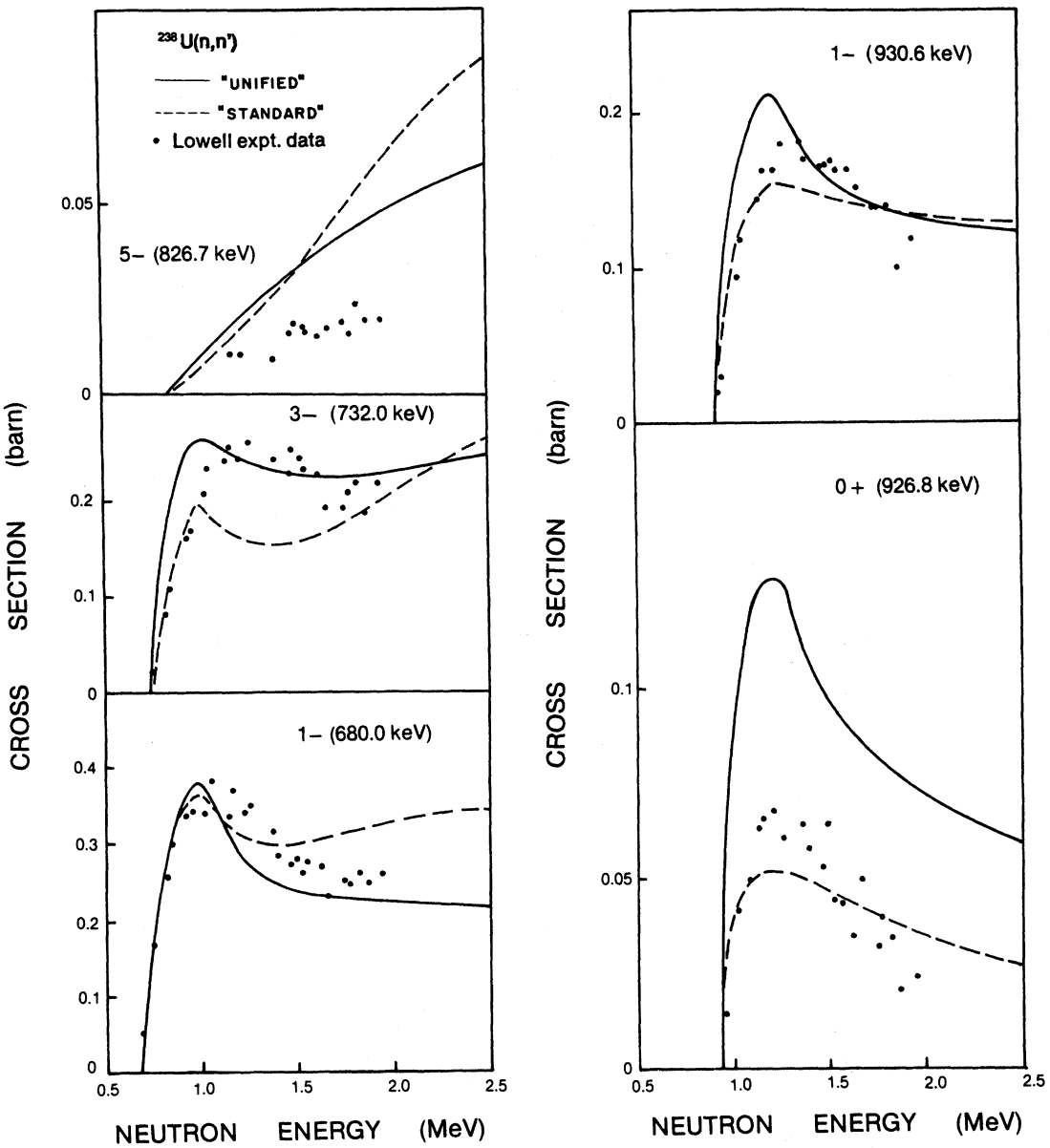

FIG. 6. Theoretical and experimental excitation functions for $^{238}U(n,n')$ inelastic scattering to levels between 680.0 and 930.6 keV excitation energy (members of the $K=0^-$ octupole, 0^+ γ-vibrational quadrupole, and 1^- octupole bands). The Lowell group's experimental data (dots; the error limits are indicated in the corresponding diagrams of paper I) are contrasted with theoretical unified (solid) curves and with the predictions of the standard (CN + DI) approach (broken curves), obtained from coupled-channel computations. The calculated numerical data are listed in Table II.

tainment of an optimal fit. The values, as cited in Tables I and II, do not necessarily correspond with those that yielded a best fit for the standard approach, but in general are not appreciably different. In all instances where they appear to differ [except for the 930.8-keV (1^-) level in ^{238}U], the "unified" coupling strengths are the smaller of the two. No very exhaustive attempt was made to vary or "fine tune" the coupling strengths, in view of the lengthy running times that the unified calculations necessitated.

For the six ^{232}Th analyses in Fig. 2, the unified results surpass the standard results in four instances; only for the data displayed at bottom and center left [i.e., the lowest-lying residual levels, 714.2 keV (1^-) and 730.3 keV (0^+)] do the unified

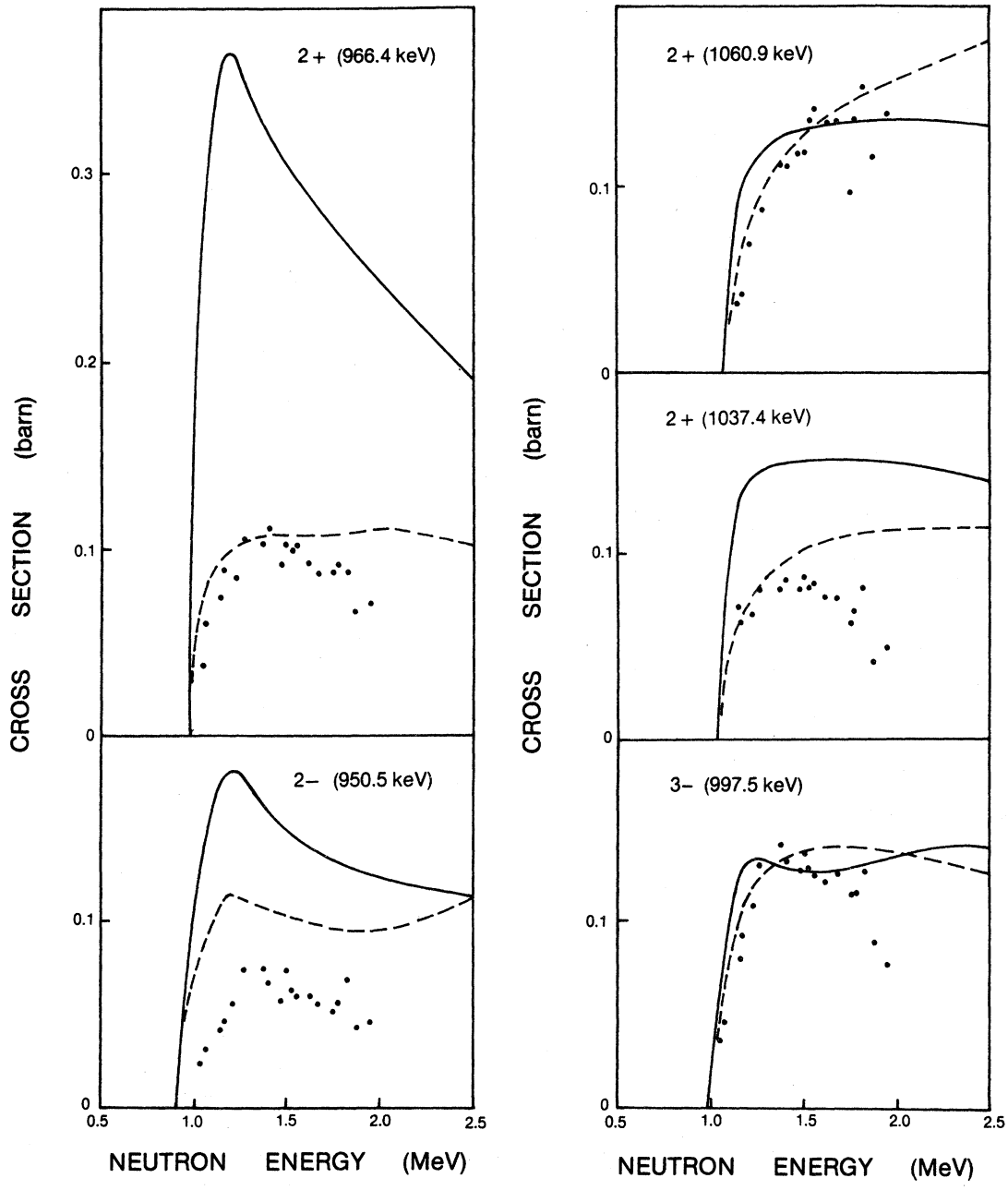

FIG. 7. Same as Fig. 6, but for ^{238}U levels between 950.5 and 1060.9 keV that are members of the $K=1^-$ octupole, 0^+ γ-vibrational, 0^+ β-vibrational, and 2^+ γ-vibrational quadrupole bands.

(solid) curves not conform as closely to the measurements as do the standard (broken) curves. In both instances, although the unified cross sections are somewhat too high in magnitude, the drop in the magnitude with increasing energy evinces the correct trend. In this and in the subsequent figures, the error limits on the experimental data have been shown in paper I: They vary from case to case, but in general are roughly $\pm 10\%$. In Fig. 3, the unified curve conforms to the measured data even more closely than the standard curve in the sole instance [center left, 883.3-keV (5^-) level] in which a satisfactory fit between theory and experiment could be achieved. The remaining results are inconclusive. However, in Fig. 4 the standard approach provided a better match than the unified in two instances [center and upper left, 1078.4-keV (0^+) and 1105.4-keV (3^-) levels]. Similarly, in Fig. 5 the fits

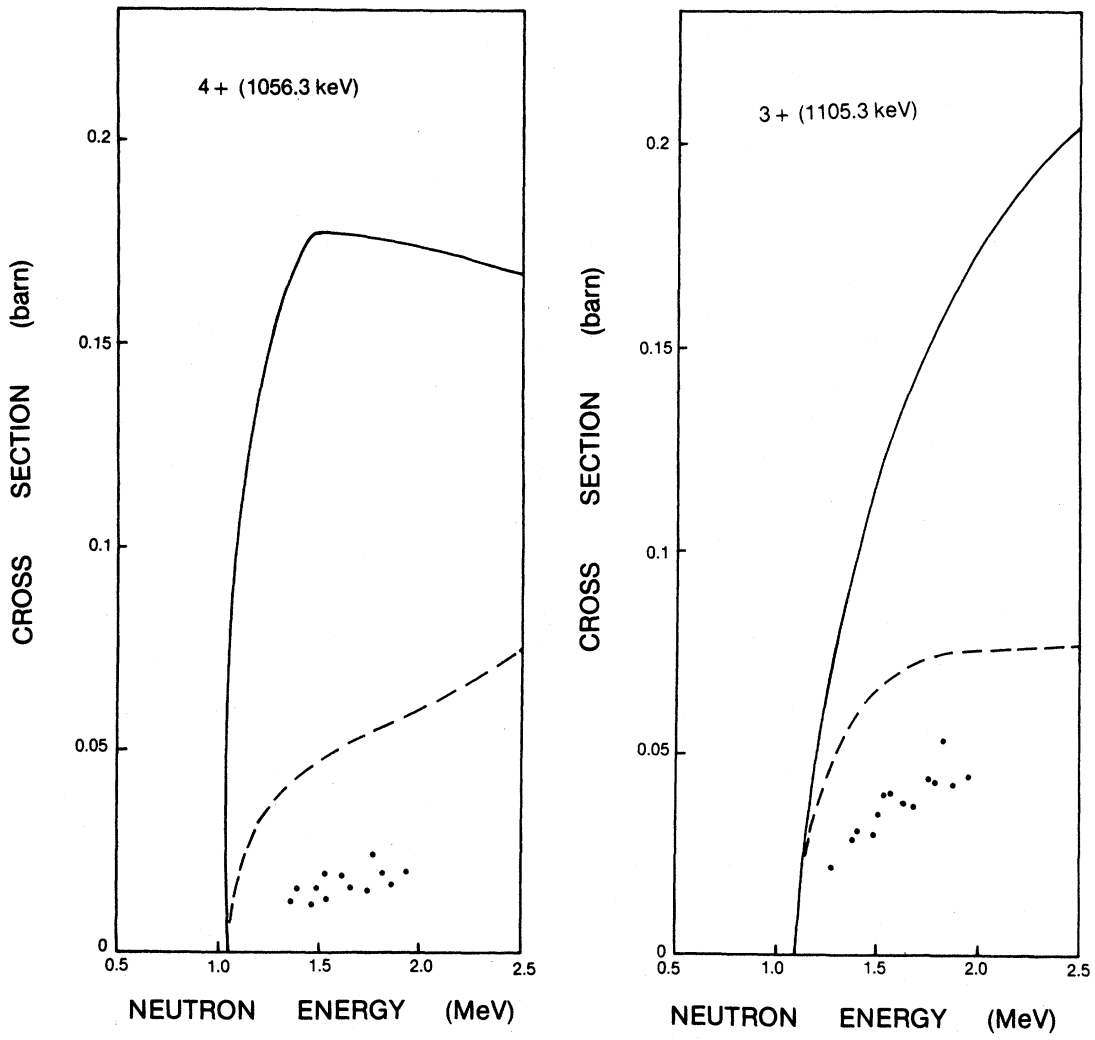

FIG. 8. Same as Fig. 6, but for the 1056.3-keV (4^+, $K=0^+$ two-phonon γ-vibrational), and 1105.3-keV (3^+, $K=2^+$ one-phonon γ-vibrational) states in ^{238}U. The anomalously small magnitude of the experimental data renders it impossible to attain a satisfactory theoretical fit with either approach.

with standard theory were superior to those from unified theory in two instances [lower left, upper right, 1143.1-keV (4^-) and 1208.7-keV (5^-) levels, respectively]. A substantial number of measured excitation functions could not be fitted by any theoretical approach; the experimental data in some instances are suspect.

The ^{238}U(n,n') analyses in Figs. 6—9 evinced a roughly similar showing. In Fig. 6, three cases manifested a superior fit with unified theory, one case with standard theory, and one case with neither. In Fig. 7, the unified approach led to a more convincing fit in one instance [top right, 1060.9-keV (2^+) level], and the standard approach in another [top left, 966.4-keV (2^+) level]. Neither seemed to be capable of reproducing the drop in cross section with increasing incident energy beyond the peak. In Fig. 8, the experimental cross sections were so small that neither approach could provide a fit. In Fig. 9, a satisfactory fit could be procured with the unified approach in fitting the 1128.9-keV level data for either spin assignment (4^+ or 2^-, lower and center left, respectively; however, the standard analysis indicated the latter assignment to be preferable). A somewhat inferior fit ensued with unified theory in the case of the 1167.4-keV (4^+) level (top left), and a somewhat superior match resulted for the 1269.4-keV (6^+) level (top right). In the remaining two cases, the experimental data were too low to admit of either approach.

Regarded overall, the unified theory has a better record of success in fitting the experimental ^{232}Th

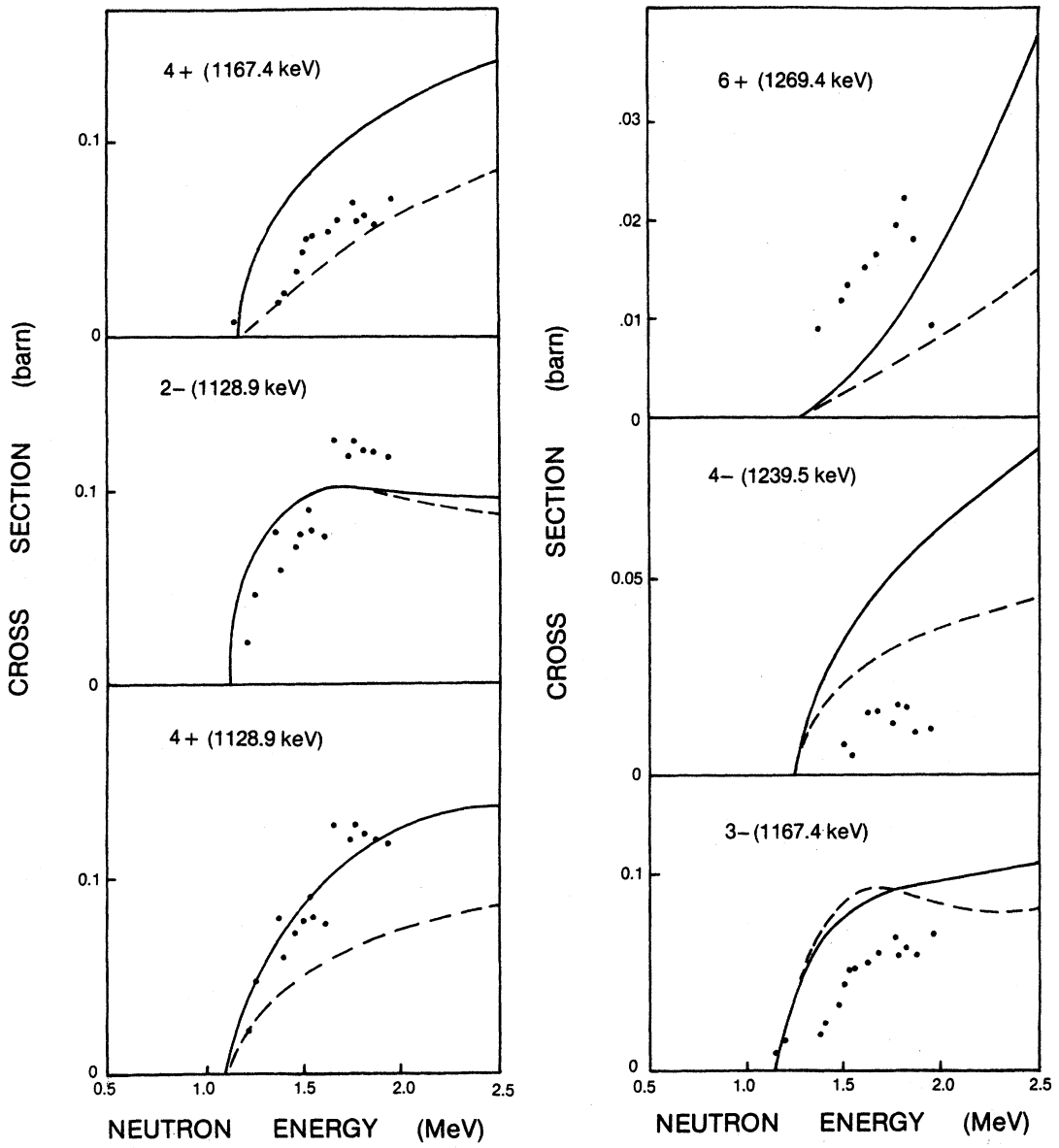

FIG. 9. Same as Fig. 6, but for ^{238}U levels between 1128.9 keV (for which two spin-parity assignments have been examined) and 1269.4 keV, that are members of the $K=0^+$ β-vibrational, 2^- octupole, and 2^+ γ-vibrational bands.

and ^{238}U data than the standard theoretical approach; it has, moreover, better fundamental justification. In the main, it has the tendency to overestimate the magnitude of the cross section, an effect which becomes particularly evident when data for several levels are combined, as in the evaluated neutron data files (ENDF/B-V). In these, cross-section data for all levels within a given excitation energy region have been combined within a composite in order to conserve the limited file storage capacity. Consequently, the totality of data assembled in papers I and II (cited in Tables I and II) reduce to just eight composite cases for ^{232}Th and six for ^{238}U. The results and level combinations are presented in Tables III and IV, and displayed in Figs. 10–13.

The curves from evaluated ENDF/B-V data[45–48] all have the same characteristic shape: After rising steeply to a peak they drop quite rapidly with increasing energy, manifesting a skewed bell shape. This rapid dropoff is not exhibited by the measured data in general, and is not reproducible with either the unified or the standard calculations. Thus, in Fig. 10 for ^{232}Th, the unified composite cross section (curve "*U*") diminishes with energy only in one

TABLE III. ^{232}Th (n,n') combined cross sections (in mb) for composite groups of levels, derived from standard and unified formalisms with the Haouat-Lagrange optical potential and deformation parameters and compared with the evaluated ENDF/B-V excitation function from 0.8 to 2.5 MeV.

ENDF/B-V effective composite energy E^* (keV)	Number of levels	Ensemble of levels	Data approach	$\sigma(n,n')$ in mb for neutron energy 0.8	1.0	1.2	1.5	2.0	2.5 MeV
725.1	2	a	Standard	196	328	308	275	286	310
	2	a	Unified	322	527	458	348	303	276
	2	a	ENDF/B-V	260	392	340	220	110	60
796.4	4	b	Standard	32	608	683	658	624	634
	4	b	Unified	128	984	1033	929	962	974
	4	b	ENDF/B-V	40	820	795	593	320	170
886.1	3	c	Standard		74	125	146	189	240
	3	c	Unified		89	180	240	337	369
	3	c	ENDF/B-V		95	150	140	100	70
954.4	1	d	Standard		3	7	16	25	31
	1	d	Unified		6	35	49	82	100
	1	d	ENDF/B-V		17	40	41	30	25
1086	6	e	Standard			275	491	453	480
	6	e	Unified			484	788	720	686
	6	e	ENDF/B-V		170	420	462	285	180
1142	2	f	Standard			33	84	128	135
	2	f	Unified			37	182	222	256
	2	f	ENDF/B-V			130	258	146	90
1187	1	g	Standard			2	101	150	141
	1	g	Unified			6	86	106	116
	1	g	ENDF/B-V			10	96	48	24
1218	2	h	Standard				38	58	74
	2	h	Unified				55	105	146
	2	h	ENDF/B-V				90	38	29

[a]Comprises the 714.3 (1^-) and 730.4 (0^+) levels.
[b]Comprises the 774.1 (2^-), 774.4 (3^-), 785.2 (2^+), and 829.6 (3^+) levels.
[c]Comprises the 873.0 (4^+), 883.3 (5^-), and 890.1 (4^+) levels.
[d]Comprises the 960.2 (5^+) level.
[e]Comprises the 1053.6 (2^-), 1077.5 (1^-), 1078.7 (0^+), 1094.4 (2^-), 1105.7 (3^-), and 1122.8 (2^+) levels.
[f]Comprises the 1143.3 (4^-) and 1147.9 (4^+) levels.
[g]Comprises the 1182.5 (3^-) level.
[h]Comprises the 1208.9 (5^-) and 1218.1 (4^-) levels.

instance (lower left, 725.1-keV composite data), while the standard cross section (curve "*S*") increases beyond $E_n \simeq 1.5$ MeV in all cases. The composite experimental data (dots) are in all instances in disaccord with the evaluation (curve "*E*"), but in three out of the four cases are satisfactorily fitted by the standard curves (*S*), whereas the unified curves (*U*) on the right-hand side evince an anomalously steep rise with energy. In Fig. 11, no close fits over the entire energy range are evident. In Fig. 12 for ^{238}U, the evaluation (*E*) fits the data well in the two upper cases and fairly closely in one further case (lower left), but is in crass disaccord with the remaining case (lower right), in which the experimental data are anomalously low. It is arguable, though, that the unified curves (*U*) offer about as good a fit in the two left-hand cases. It also bears pointing out that for the upper right-hand case (968.8-keV effective composite energy) the high-magnitude unified curve was obtained by summing over six levels, whereas the experimental data were a composite of measurements for five levels only. In Fig. 13, no close fits are discernible, though in the lower left-hand figure (1052-keV effective composite energy) both the unified (*U*) and evaluated (*E*) curves appear to be in accord with the experimental data. For the upper left case (1175-keV effective composite energy), the high-

TABLE IV. $^{238}U(n,n')$ combined cross sections (in mb) for composite groups of levels, derived from standard and unified formalisms with the Haouat-Lagrange optical potential and deformation parameters and compared with the evaluated ENDF/B-V excitation function from 0.8 to 2.5 MeV.

ENDF/B-V effective composite energy E^* (keV)	Number of levels	Ensemble of levels	Data approach	$\sigma(n,n')$ in mb for neutron energy 0.8	1.0	1.2	1.5	2.0	2.5
							MeV		
682.7	1	a	Standard	275	366	302	289	331	345
	1	a	Unified	266	356	278	234	226	219
	1	a	ENDF/B-V	216	328	260	174	87	35
734.9	1	b	Standard	39	178	149	144	203	261
	1	b	Unified	126	267	246	225	233	239
	1	b	ENDF/B-V	66	239	255	189	93	38
830.3	1	c	Standard		6	14	28	66	85
	1	c	Unified		9	19	30	49	60
	1	c	ENDF/B-V		25	100	100	54	41
968.8	6	d	Standard		187	557	574	585	612
	6	d	Unified		366	1099	886	771	691
	6	e	ENDF/B-V		144	505	495	373	275
1052	3	f	Standard			186	284	317	371
	3	f	Unified			377	460	457	441
	3	f	ENDF/B-V			290	468	385	259
1175	5	g	Standard			130	353	373	409
	5	g	Unified			168	465	573	631
	4	h	ENDF/B-V			56	331	266	235
1255	7	i	ENDF/B-V				150	175	87
1446	8	j	ENDF/B-V				110	290	185

[a]Comprises the 680.0 keV (1^-) level.
[b]Comprises the 731.9 keV (3^-) level.
[c]Comprises the 827.2 keV (5^-) level.
[d]Comprises the 927.2 (0^+), 930.8 (1^-), 950.0 (2^-), 966.3 (2^+), 993.0 (0^+), and 997.5 keV (3^-) levels.
[e]Comprises the 927 (0^+), 931 (1^-), 950 (2^-), 966 (2^+), 997 (0^+), and 997 keV (3^-) levels. Composite experimental data from the 927.2 (0^+), 930.8 (1^-), 950.0 (2^-), 966.3 (2^+), and 997.5 keV (3^-) levels.
[f]Comprises the 1037.3 (2^+), 1055.0 (4^+), and 1060.9 (2^+) levels. Composite experimental data from the 1037.3 (2^+), 1055.0 (4^+), 1059.9 (?), and 1060.9 keV (2^+) levels.
[g]Comprises the 1105.3 (3^+), 1127.0 (4^+), 1128.9 (2^-), 1167.4 (4^+), and 1169.4 keV (3^-) levels.
[h]Comprises the 1105.3 (3^+), 1128.9 (2^-), 1167.4 (4^+), and 1209 keV (4^-) levels. Composite experimental data from the 1105.3 (3^+), 1128.9 (2^-), and 1167.4 keV (4^+) levels.
[i]Comprises the 1224 (2^+), 1243 (4^-), 1261 (?), 1269.4 (6^+), 1279 (?), 1309 (?), and 1381 keV (?) levels. Composite experimental data from the 1224.0 (?), 1243 (4^-), 1260.5 (?), 1269.4 (6^+), 1279.2 (?), 1308.5 (?), and 1381.1 keV (?) levels.
[j]Comprises the 1413 (?), 1437 (?), 1446 (?), 1455 (?), 1516 (?), and 1561 keV (?) levels. Composite experimental data from the 1413.2 (?), 1437.4 (?), 1446.2 (?), 1455.2 (?), 1515.7 (?), and 1561 keV (?) levels.

magnitude unified (U) and standard (S) curves ensued from summation over five sets of data, whereas the evaluated curve (E) was a composite of only four sets, and the experimental data a composite of but three sets. In the two cases on the right, it was not possible to include unified (U) or standard (S) curves as the computations could not be carried to high-excitation levels whose spins and parities were not known. In the diagram on the upper right, the existence of an experimental point at the lowest energy apparently below the threshold [i.e., to the left of the evaluation curve (E)] is no error: The data were obtained from scattering to levels lying within about 150 keV on either side of the effective energy $E^*=1446$ keV; hence the effective threshold energy is roughly $E_n \simeq 1.3$ MeV (a similar explanation applies to the two lowest dots on the upper right of Fig. 12).

From a critique of the entire batch of results, one would have to conclude that an evident need exists

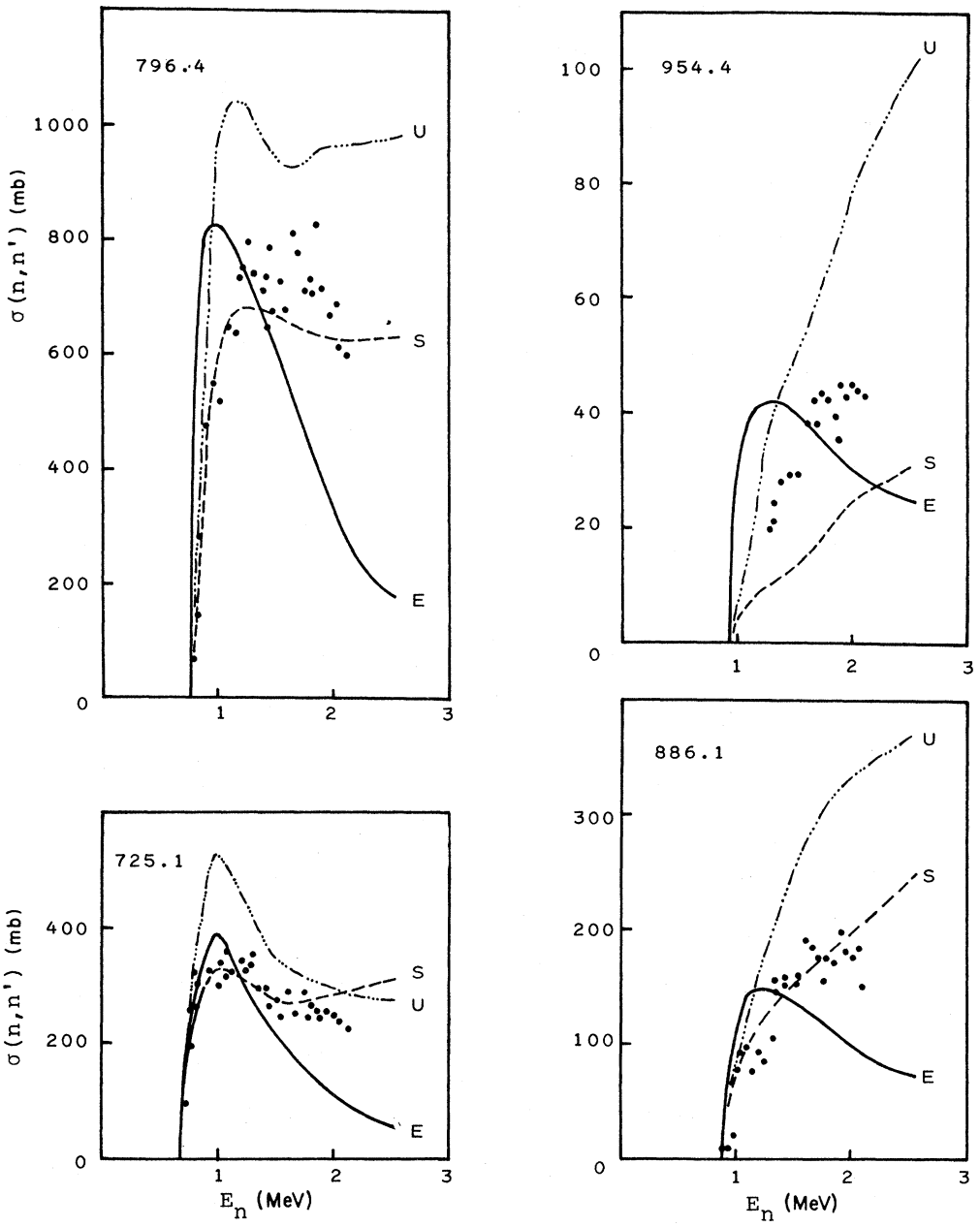

FIG. 10. Comparison, against the Lowell group's composite (n,n') experimental data (dots), of the computed unified (U curves), standard (S curves), and ENDF/B-V evaluated (E curves) excitation functions for combined groups of ^{232}Th levels as indicated in the numerical tabulation in Table III.

for an upward revision of the ENDF/B-V evaluated cross sections at incident energies beyond the peak. The present trend appears to take insufficient cognizance of the onset of direct scattering beyond $E_n \simeq 1.5$ MeV: The DI admixture furnishes a substantial and growing contribution thereafter—indeed, one that increases somewhat too drastically in several instances, if the evidence of standard and unified composite functions is taken as a guide. The fact that in seven out of the 16 cases shown in Figs. 10—13 the unified cross sections above $E_n = 2.0-2.5$ MeV continue their steep rise suggests

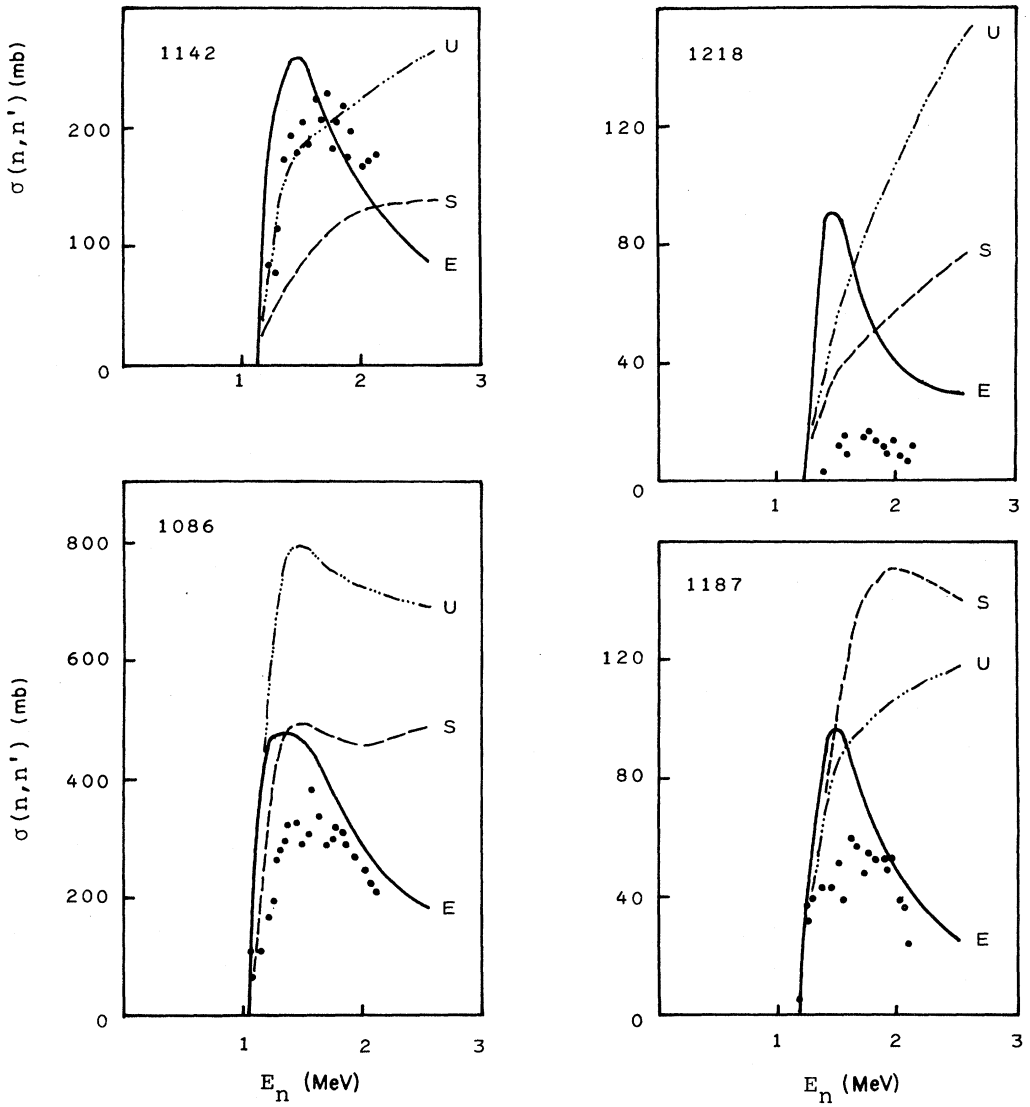

FIG. 11. Same as Fig. 10, but for the higher-lying composite groups of ^{232}Th levels.

that correction procedures to drain some of the DI strength through additional competing channels should be introduced into the intrinsic unified treatment. Ancillary investigations including radiative capture and continuum competition in the computations confirmed the expectation that these channels exert only a rather slight influence upon the outcome in the case[49] of ^{232}Th: Their effect is experienced mainly in the threshold region, just as is the Moldauer level-width fluctuation correction. Nevertheless, it is planned to incorporate these options within the program NANCY (the procedures cannot simply be taken over from CINDY, since the latter entails intensity addition while NANCY operates with amplitude addition). More importantly, it is intended that provision for fission channels be included in NANCY; fission competition is expected to produce a perceptible effect in the 2.0–2.5 MeV region for the fertile even-A nuclei such as ^{232}Th and ^{238}U [the calculated[49] fission cross section for ^{232}Th $+n$ peaks at 2.18 MeV and its value, $\sigma(n,f)=137$ mb, is appreciable in comparison with the inelastic magnitudes featured in Figs. 10–13]. For future investigations, the inclusion of a fission correction is essential, and particularly so for any studies of neutron scattering interactions

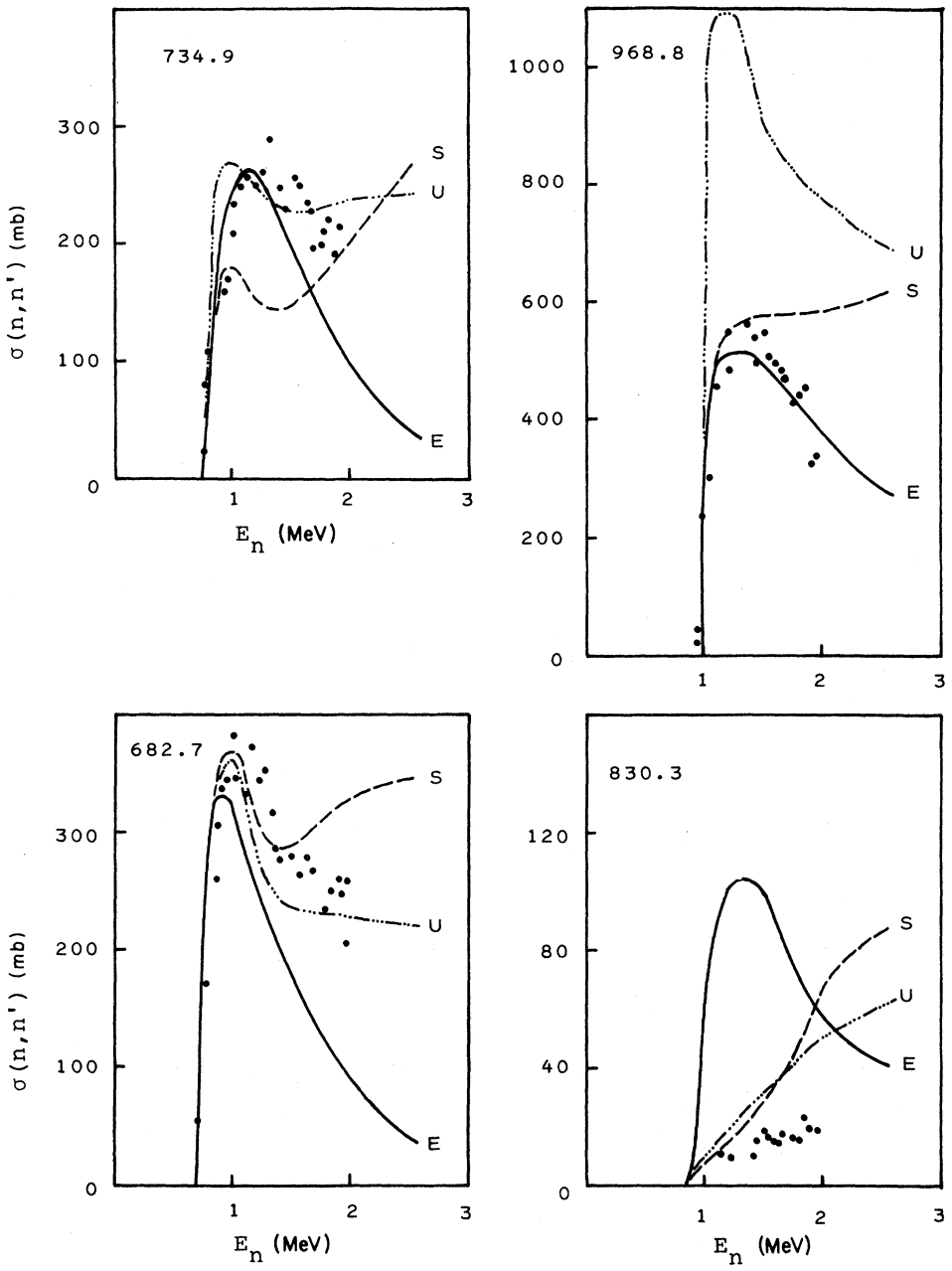

FIG. 12. Same as Fig. 10, but for lower-lying groups of levels in ^{238}U, as indicated in Table IV. The conspicuously high magnitude of the unified curve (*U*) in the upper right-hand side is attributable to the fact that data for six levels were combined to obtain the theoretical curves, whereas the experimental dots refer to the summed data from only five levels.

with fissile odd-*A* actinide nuclei. The exploration of such extensions to the unified approach will form the subject of a later paper (paper III).

Meanwhile, the evaluated ENDF/B-V file data for inelastic neutron scattering from ^{232}Th and ^{238}U might conceivably also be revised. In the evaluation procedures, primary weight is given to attaining as close a match as possible to measured total and elastic neutron cross sections in each instance: From the difference of these two comparatively large magnitudes, the relatively small residual inelastic cross section is deduced. It would require only a small concession in the goodness of fit to elastic data to bring the inelastic component into agreement with experiment and calculation. This restoration of the inelastic cross section in an impor-

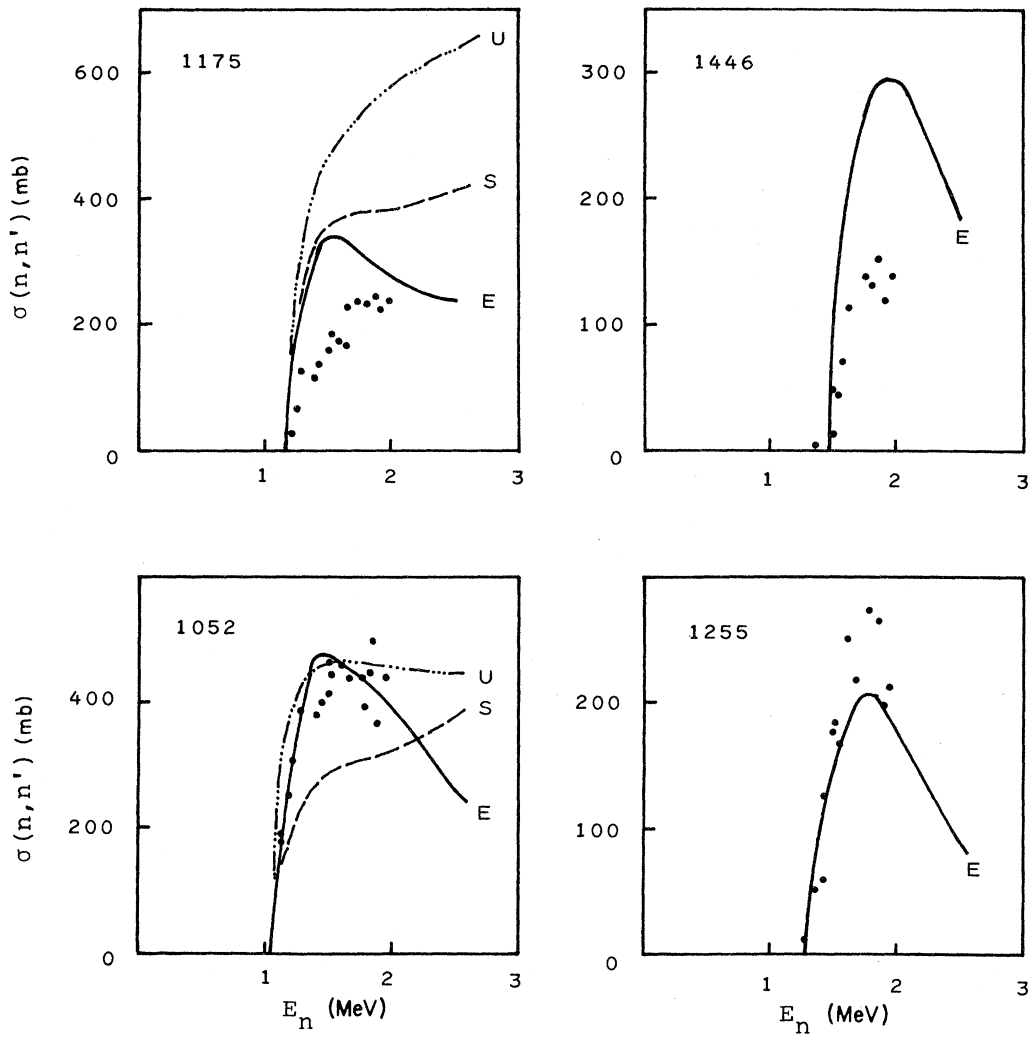

FIG. 13. Same as Fig. 10, but for the higher-lying groups of levels in ^{238}U. In the two right-hand diagrams, computations could not be carried out to obtain theoretical data, since the levels were at too high an excitation energy to permit reliable spin, parity, or band assignments to be made. Thus, only the ENDF/B-V evaluated data, as listed in Table IV, have been used for comparison.

tant data base would have desirable consequences in regard to the nuclear engineering and physics problems associated with the design and operation of fast reactors, since inelastic scattering comprises the main determinant of the energy distribution in the neutron flux spectrum. The establishment of an accurate and reliable data base in fine detail continues to call for improvement in all three domains: the refinement and consolidation of experimental data acquisition procedures, the further development of precision and definitiveness in the theoretical predictions, and the adjustment of data evaluations to reflect the ongoing improvement in knowledge. The unified approach, even in its intrinsic unembellished form as explored in the present investigation, offers valuable progress in the quest for a definitive, comprehensive theoretical description, in all its diversity, intricacy, and complexity.

ACKNOWLEDGMENTS

The results presented herein formed the basis for a thesis in partial fulfillment of the requirements for the conferment (upon D.W.S.C.) of a Ph.D. degree by the University of Lowell. The data have been deposited with the National Neutron Cross Section Center at the Brookhaven National Laboratory. For the facilities to pursue these investigations, Dr. L. E. Beghian and the University administration are thanked, and in particular we ack-

nowledge with gratitude the generous cooperation of Dr. S. C. Mathur (Director) and the staff of the University Computation Center. For helpful and enlightening discussions, and for the provision of unpublished material, appreciation is expressed to Dr. Hofmann, Dr. Kretschmer, Dr. Moldauer, Dr. Tepel, and Dr. Weidenmüller, as well as to Dr. Hausman, Dr. Moldauer, Dr. Rapaport, and Dr. Raynal for making computer routines and programs available to us. The use of the Lowell group's experimental data is appreciatively acknowledged. This research was supported in part by grants from the U.S. National Science Foundation and the Department of Energy.

---

*Present address: General Physics Corporation, 1000 Century Plaza, Columbia, MD 21044.

[1]D. W. S. Chan, J. J. Egan, A. Mittler, and E. Sheldon, Phys. Rev. C 26, 841 (1982).

[2]B. Baldoni and A. M. Saruis, Nuovo Cimento 33, 1145 (1964).

[3]J. J. Egan, G. H. R. Kegel, G. P. Couchell, A. Mittler, T. V. Marcella, N. B. Sullivan, E. Sheldon, and A. Prince, in *Nuclear Cross Sections and Technology (Proceedings of a Conference, Washington, D. C., 1975),* edited by R. A. Schrack and C. D. Bowman, National Bureau of Standards Special Publication NBS SP-425, 1975, Vol. II, p. 950.

[4]E. Sheldon and V. C. Rogers, Comput. Phys. Commun. 6, 99 (1973).

[5]T. Tamura, Oak Ridge National Laboratory Report ORNL-4152, 1967; Rev. Mod. Phys. 37, 679 (1965).

[6]H. Rebel and G. W. Schweimer, Kernforschungszentrum Karlsruhe Report KFK-1333, 1971.

[7]G. Haouat, Ch. Lagrange, J. Lachkar, J. Jary, Y. Patin, and J. Sigaud, in *Nuclear Cross Sections for Technology, Proceedings of the International Conference, University of Tennessee, Knoxville, 1979,* edited by J. L. Fowler, C. H. Johnson, and C. D. Bowman, National Bureau of Standards Special Publication NBS SP-594 1980, p. 672.

[8]C. A. Engelbrecht and H. A. Weidenmüller, Phys. Rev. C 8, 859 (1973).

[9]J. W. Tepel, H. M. Hofmann, and H. A. Weidenmüller, Phys. Lett. 49B, 1 (1974).

[10]H. M. Hofmann, J. Richert, J. W. Tepel, and H. A. Weidenmüller, Ann. Phys. (N.Y.) 90, 391 (1975); 90, 403 (1975).

[11]D. W. S. Chan, Ph.D. thesis, University of Lowell, 1981.

[12]H. M. Hofmann, T. Mertelmeier, M. Herman, and J. W. Tepel, Z. Phys. A 297, 153 (1980).

[13]G. Graw, H. Clement, J. H. Feist, W. Kretschmer, and P. Pröschel, Phys. Rev. C 10, 2340 (1974).

[14]P. Pröschel, Diploma dissertation, University of Erlangen-Nürnberg, 1975.

[15]H. Clement, Ph.D. dissertation, University of Erlangen-Nürnberg, 1974.

[16]P. D. Kunz, private communication.

[17]E. Sheldon, Nukleonika 26, 471 (1981).

[18]C. Mahaux, in *Statistical Properties of Nuclei,* Proceedings of the International Conference on the Statistical Properties of Nuclei, Albany, 1971, edited by J. B. Garg (Plenum, New York, 1972), p. 545.

[19]C. Mahaux, Fizika (Zagreb), Suppl. 2, 11, 21 (1979).

[20]W. Kretschmer and G. Graw, Phys. Rev. Lett. 27, 1294 (1971).

[21]J.-H. Feist, Ph.D. dissertation, University of Erlangen-Nürnberg, 1975.

[22]K. P. Lieb, J. J. Kent, and C. F. Moore, Phys. Rev. 175, 1482 (1968).

[23]R. Albrecht, K. Mudersbach, J. P. Wurm, and U. Zoran, in *Proceedings of the International Conference on Nuclear Physics, Munich, 1973,* edited by J. de Boer and H. J. Mang (North-Holland, New York, 1973), p. 577.

[24]S. L. Davis, Ph.D. thesis, Rutgers University, 1974.

[25]S. Davis, C. Glashausser, A. B. Robbins, G. Bissinger, R. Albrecht, and J. P. Wurm, Phys. Rev. Lett. 34, 215 (1975).

[26]V. A. Konshin, in *Nuclear Theory for Applications—1980,* Proceedings of the Interregional Advanced Training Course on Applications of Nuclear Theory to Nuclear Data Calculations for Reactor Design, Trieste, 1980 (International Center for Theoretical Physics, Trieste, 1981), p. 139.

[27]V. Stavinsky and M. O. Shaker, Nucl. Phys. 62, 667 (1965).

[28]J. E. Lynn, Phys. Lett. 18, 31 (1965).

[29]D. Shackleton, J. Trochon, and J. Frehaut, in *Proceedings of the International Conference on Physics and Chemistry of Fission, Rochester, 1973* (IAEA, Vienna, 1974).

[30]J. Frehaut, D. Shackleton, and J. Trochon, in *Proceedings of the International Conference on Nuclear Physics, Munich, 1973,* edited by J. de Boer and H. J. Mang (North-Holland, New York, 1973), Vol. I.

[31]J. Trochon, in *Proceedings of the International Colloquium on the Physics and Chemistry of Fission,* Jülich, *1979* (unpublished).

[32]W. Hauser and H. Feshbach, Phys. Rev. 87, 366 (1952).

[33]G. R. Satchler, Phys. Lett. 7, 55 (1963).

[34]M. Kawai, A. K. Kerman, and K. W. McVoy, Ann. Phys. (N.Y.) 75, 156 (1973).

[35]P. A. Mello, Phys. Lett. 81B, 103 (1979).

[36]P. A. Mello and T. H. Seligman, Notas Fíz. 2, 182 (1979).

[37]P. A. Mello, Fizika (Zagreb) Suppl. 2, 11, 33 (1979).

[38]P. A. Mello, Notas Fís. 3, 189 (1980).
[39]P. A. Mello and T. H. Seligman, Nucl. Phys. A344, 489 (1980).
[40]W. R. Smith, Comput. Phys. Commun. 1, 106 (1969).
[41]B. T. Smith, J. M. Boyle, B. S. Garbow, Y. Ikebe, V. C. Klemma, and C. B. Møler, *Matrix Eigensystem Routines* (Springer, New York, 1974).
[42]P. A. Moldauer, in *Nuclear Theory for Applications,* Proceedings of the Course on Nuclear Theory for Applications, Trieste, 1978 (International Centre for Theoretical Physics, Trieste, 1980), p. 165.
[43]J. H. Dave, J. J. Egan, G. P. Couchell, G. H. R. Kegel, A. Mittler, D. J. Pullen, W. A. Schier, and E. Sheldon, Phys. Rev. C (to be published).
[44]A. Mittler *et al.*, Phys. Rev. C (to be published).
[45]J. Meadows, W. Poenitz, A. Smith, D. Smith, J. Whalen, and R. Howerton, Argonne National Laboratory Report ANL/NDM-35, 1978.
[46]J. W. Meadows, W. P. Poenitz, A. B. Smith, D. L. Smith, J. F. Whalen, R. J. Howerton, B. R. Leonard, G. de Saussure, R. L. Macklin, R. Gwin, and M. R. Bhat, Evaluated Nuclear Data File-B, Version V (ENDF/B-V) (for ^{232}Th), MAT 1390, National Neutron Cross Section Center, Brookhaven National Laboratory, 1979.
[47]W. Poenitz, E. Pennington, A. B. Smith, and R. Howerton, Argonne National Laboratory Report ANL/NDM-32, 1977.
[48]E. Pennington, A. Smith, W. Poenitz, and M. R. Bhat, Evaluated Nuclear Data File-B, Version V (ENDF/B-V) (for ^{238}U), MAT 1395, National Neutron Cross Section Center, Brookhaven National Laboratory, 1977 and 1980.
[49]H. Abou Yehia, J. Jary, and J. Trochon, Bruyères-le-Châtel Report NEANDC (E) 204 "L," INDC (FR) 34/L, 1979.
[50]E. Sheldon and D. W. S. Chan, in Proceedings of the Organization for Economic Co-operation and Development (OECD) [Nuclear Energy Agency, Nuclear Data Committee (NEANDO)] Specialists' Meeting on Fast Neutron Scattering on Actinide Nuclei, Paris, 1982 (to be published).